cy. 2

DROPLET DIAMETER AND SIZE DISTRIBUTION OF JP-4 FUEL INJECTED INTO A SUBSONIC AIRSTREAM

R. A. Wasson, Jr., C. R. Darlington, and J. C. Billingsley
ARO, Inc.

ENGINE TEST FACILITY
ARNOLD ENGINEERING DEVELOPMENT CENTER
AIR FORCE SYSTEMS COMMAND
ARNOLD AIR FORCE STATION, TENNESSEE 37389

April 1975

Final Report for Period October 22, 1973 — December 12, 1973

This report has been reviewed by the Information Office (OI) and is releasable to the National Technical Information Service (NTIS). At NTIS, it will be available to the general public, including foreign nations.

APPROVAL STATEMENT

This technical report has been reviewed and is approved for publication.

FOR THE COMMANDER

EULES L. HIVELY
Research and Development
 Division
Directorate of Technology

ROBERT O. DIETZ
Director of Technology

REPORT DOCUMENTATION PAGE

READ INSTRUCTIONS
BEFORE COMPLETING FORM

1. REPORT NUMBER	2. GOVT ACCESSION NO.	3. RECIPIENT'S CATALOG NUMBER
AEDC-TR-74-117		

4. TITLE (and Subtitle)	5. TYPE OF REPORT & PERIOD COVERED
DROPLET DIAMETER AND SIZE DISTRIBUTION OF JP-4 FUEL INJECTED INTO A SUBSONIC AIRSTREAM	Final Report-October 22, 1973-December 12, 1973
	6. PERFORMING ORG. REPORT NUMBER

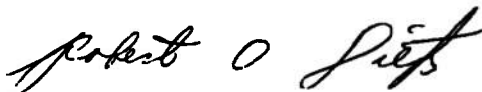| 7. AUTHOR(s)	8. CONTRACT OR GRANT NUMBER(s)
R. A. Wasson, Jr., C. R. Darlington, and J. C. Billingsley, ARO, Inc.	

9. PERFORMING ORGANIZATION NAME AND ADDRESS	10. PROGRAM ELEMENT, PROJECT, TASK AREA & WORK UNIT NUMBERS
Arnold Engineering Development Center Arnold Air Force Station, Tennessee 37389	Program Element 62601F Project 1900

11. CONTROLLING OFFICE NAME AND ADDRESS	12. REPORT DATE
Arnold Engineering Development Center (DYFS) Arnold Air Force Station, Tennessee 37389	April 1975
	13. NUMBER OF PAGES
	41

14. MONITORING AGENCY NAME & ADDRESS(if different from Controlling Office)	15. SECURITY CLASS. (of this report)
	UNCLASSIFIED
	15a. DECLASSIFICATION/DOWNGRADING SCHEDULE N/A

16. DISTRIBUTION STATEMENT (of this Report)

Approved for public release; distribution unlimited.

17. DISTRIBUTION STATEMENT (of the abstract entered in Block 20, if different from Report)

18. SUPPLEMENTARY NOTES

Available in DDC

19. KEY WORDS (Continue on reverse side if necessary and identify by block number)

drop
sizes   subsonic flow
distribution   holograms
JP-4 fuel   altitude

20. ABSTRACT (Continue on reverse side if necessary and identify by block number)

A test program was conducted to determine the size and distribution of JP-4 fuel droplets when fuel was dispersed at a constant fuel nozzle exit velocity into a subsonic airstream. Testing was conducted at free-stream flight velocities ranging from 200 to 400 knots at altitudes ranging from 12,000 to 25,000 feet with flow rates of approximately 13, 75, and 290 lbm/min. Holograms of the fuel droplets were taken 18 feet downstream of

DD FORM 1473 1 JAN 73   EDITION OF 1 NOV 65 IS OBSOLETE

20. ABSTRACT (Continued)

the fuel nozzle exit plane. Representative histograms of fuel droplet size distribution and average fuel droplet diameter are presented. Average fuel droplet diameter was not significantly affected by any of the test variables. All arithmetic average fuel droplet diameter data were within a 19- to 36-micron band.

AFSC
Arnold AFS Tenn

PREFACE

The work reported herein was a portion of the Control of Noxious Effluents (CONE) Program, sponsored by the Air Force Weapons Laboratory, Kirtland AFB, New Mexico. The work was performed under Program Element 62601F and Air Force Project Number 1900. The tests were conducted in the Propulsion Research Area (R-2B), Engine Test Facility (ETF), Arnold Engineering Development Center (AEDC), Air Force System Command (AFSC), Arnold Air Force Station, Tennessee. The test was conducted from October 22, 1973 to December 12, 1973, and the data analysis was completed on March 1, 1974. The results of the test were obtained by ARO, Inc. (a subsidiary of Sverdrup & Parcel and Associates, Inc.), contract operator of AEDC, Arnold Air Force Station, Tennessee, under ARO Project No. VF460. The manuscript (ARO Control No. ARO-ETF-TR-74-92) was submitted for publication on September 30, 1974.

CONTENTS

ILLUSTRATIONS

TABLES

1.0 INTRODUCTION

During the flight of jet aircraft, it may be necessary to jettison JP-4 fuel. The test program reported herein was conducted as a portion of an overall program to determine the effects that the dumping of large quantities of fuel has upon the local environment.

Test program objectives were to determine the size and distribution of fuel droplets as a function of flight velocity, altitude, fuel flow rate, fuel temperature, and fuel nozzle injection angle when fuel was dispersed at a constant fuel nozzle exit velocity of 11 ± 0.5 ft/sec into a subsonic airstream. Testing was conducted at free-stream flight velocities ranging from 200 to 400 knots at altitudes ranging from 12,000 to 25,000 feet. Fuel was dispersed into the subsonic airstream at fuel flow rates of approximately 13, 75, and 290 lbm/min. Holograms to record fuel droplets were taken with a ten-megawatt, pulsed ruby laser in-line holography system.

The JP-4 fuel droplet data are presented in this report as average droplet diameter as a function of airstream velocity and altitude, for various fuel flow rates, fuel nozzle sizes, injection angles, and fuel temperatures. The average droplet diameters were calculated using three different methods. Typical fuel droplet size histograms showing droplet size distributions at nine combinations of airstream velocity, altitude, and fuel flow rate are also presented. Comparisons of the JP-4 fuel data are made with previously published results for various liquids injected into airstreams.

The program reported herein was a phase of an overall program being conducted at the AEDC to provide an initial evaluation of the impact of a fuel jettisoned on the environment and to provide guidelines which can lead to recommendations of procedures which will minimize any adverse effects that may be determined. The determination of the local and regional effects of fuel jettisoned into the atmosphere require a knowledge of the fluid injected, its physical state after injection, its residence time and influence, and the long-term photochemical interactions which may occur. The overall program includes:

1. A comprehensive literature survey to define the range of chemical and physical properties of JP-4 fuel, the dispersal and evaporation of the fuel subsequent to its injection into the atmosphere, and the state-of-the art in determining the impact of the fuel on the photochemical reactions already occurring in the atmosphere;

2. An experimental program to supplement the available information on droplet breakup and evaporation;

3. A study of the physical effects of JP-4 on the normal atmospheric processes of condensation and evaporation of water (clouds, fogs, etc); and

4. An experimental program to define the impact of JP-4 fuel on the photochemical activity in the atmosphere.

The results presented herein are intended to supplement the available information on fuel droplet breakup when the fuel is injected into an airstream.

2.0 APPARATUS

2.1 TEST INSTALLATION

The JP-4 Fuel Dump Test program was conducted in Propulsion Research Cell (R-2B) of the Engine Test Facility (ETF) at the AEDC (Ref. 1). The test cell was adapted for use as shown in Fig. 1.

Fuel was dispersed into the subsonic airstream through four interchangeable nozzles (Fig. 2) at fuel flow rates of approximately 13, 75, and 290 lbm/min. The three straight nozzles were designed to produce nozzle exit velocities of 11 ± 0.5 ft/sec at the design fuel flow rates. The canted nozzle was made of aluminum tubing to approximate the fuel flow rate and exit velocity of the large straight nozzle but with an injection angle of approximately 22 deg to the test section centerline. Fuel was supplied to the selected fuel nozzle from a tank pressurized with gaseous nitrogen to obtain the designed fuel flow rate. The fuel supply system is shown in Fig. 3.

2.2 HOLOGRAPHY SYSTEM

2.2.1 Holography Recording System

The major components of the in-line holography system are shown in Fig. 4. The laser used in the test was a Korad® K1 pulsed ruby laser. Used in the Q switched mode, this laser can produce up to 1.0 joule of energy. Since there was little beam attenuation across the flow section of the test cell, this energy was considered adequate for properly exposed holograms. In addition to the pulsed ruby laser, a low-power CW helium-neon laser was used for aligning the system. The alignment laser was mounted so that alignment could be made through the ruby laser cavity. This also allowed the components of the system to be aligned prior to and during testing.

The hologram was recorded on Agfa-Gevaert 10E75 high-quality photographic film. The film was mounted in a film pack which had an automatic film advance controlled by the laser operator.

Protective tubes, 3.5 inches in diameter, were installed to protect the laser beam from excessive fuel droplets and other matter that would tend to scatter the beam. A one-inch gap between the ends of the tubes at the test cell centerline formed the test volume. The gap dimension was determined such that a holography system minimum resolution limit of ten microns (Ref. 2) was obtainable. On each side of the test volume, 85-micron-diameter wires were attached across the ends of the protective tubes. These two wires were used as known reference dimensions and as aids to defining the test volume boundaries in the reconstructed holograms.

2.2.2 Hologram Reconstruction System

The holograms made during the test were reconstructed on a laboratory optical bench (Fig. 5). A coherent, monochromatic, collimated light beam from a 15-milliwatt, helium-neon continuous-wave laser was used to illuminate the hologram. The 6328-Ångstrom-wavelength light was sufficiently similar to the light used in the holocamera (6943 Ångstroms) to prevent significant loss of holographic image resolution.

The hologram was movable in the vertical, horizontal, and axial directions to allow reconstruction of any portion of the test volume flow field. The end boundaries on the reconstructed cylindrical test volume were located by focusing on 85-micron-diameter wires affixed across the ends of the protective tubes. The wires were also used to calibrate the fuel droplet measuring scale on the television monitor by using the 85-micron diameter as a known reference dimension. The reconstructed image on the monitor represented a 1.2- by 1.4-millimeter plane in the test volume.

The hologram was scanned and three regions, with the best resolution and the highest concentration of fuel droplets, were selected for analysis. Each selected region was traversed across the test volume, and the fuel droplets were counted and measured. Normally, a total of 128 cubic millimeters of the test volume was analyzed for each data point. Minimum diameter resolution was ten microns.

2.3 INSTRUMENTATION

Aerodynamic instrumentation was provided to measure total and static pressures and total temperatures at the fuel injection station and at the holography station as shown in Fig. 6. Pressures and temperatures were measured in the fuel system as shown in Fig. 3. The types of measuring and recording devices and the method of calibration employed prior to and after each test period are shown in Table 1. All transducers were calibrated in the AEDC Standards Calibration Laboratory (Ref. 3) before and after the test program.

2.4 DATA ACQUISITION AND REDUCTION

All aerodynamic and fuel system data were recorded on magnetic tapes, using a high-speed analog-to-digital data acquisition system. A high-speed digital computer was used to reduce the data and tabulate it in engineering units. Airstream velocities were calculated from measured temperatures and pressures using standard isentropic relations. Altitudes were calculated using static pressure and the U. S. Standard Atmosphere, 1962 (Geopotential Altitude). In addition, selected parameters were reduced on-line and displayed in the control room on a closed-circuit television for use in setting test conditions and monitoring significant parameters.

The holography system was used to record and reconstruct holograms of the test volume. The droplets were counted and measured, and average fuel droplet sizes were calculated by

$$\bar{d} = \frac{\Sigma(nd)}{n_t} \qquad \text{Arithmetic average diameter,}$$

$$\bar{d}_m = \left[\frac{\Sigma(nd^3)}{n_t}\right]^{1/3} \qquad \text{Mass-weighted average diameter,}$$

and

$$d_o = \frac{\Sigma(nd^3)}{\Sigma(nd^2)} \qquad \text{Area-volume average diameter}$$

Fuel droplet size frequency of occurrence, indicating size distribution, was calculated by

$$\psi = \frac{n]_{d_1}^{d_2}}{n_t}$$

The estimated data uncertainties are presented in Table 1. The estimates were made in accordance with Ref. 4.

3.0 TEST PROCEDURE

Prior to each run period, all instrumentation systems were calibrated and the data acquisition system was checked for proper performance. The holography system was aligned with the continuous-wave laser source, and test holograms were made with the 10-megawatt pulse laser to ensure satisfactory operation of the system. The selected fuel nozzle was installed, the corresponding flow leg was opened, and the fuel supply tank was pressurized with nitrogen.

For each data point, the desired airstream conditions were set and allowed to stabilize. The fuel tank pressure was adjusted to the proper level and holograph laser charging was initiated. On a countdown sequence the data acquisition system was started, the fuel supply solenoid valve was opened, the holography laser was fired, the fuel supply solenoid valve was closed, and the data acquisition system was turned off. Fuel was allowed to flow for six to eight seconds, and the hologram was taken three to five seconds after the fuel supply valve was opened. The laser pulse was 30 nanoseconds in duration.

4.0 RESULTS AND DISCUSSION

Test program objectives were to determine the size and distribution of fuel droplets as a function of flight velocity, altitude, fuel flow rate, fuel temperature, and fuel nozzle injection angle when fuel was dispersed at a constant fuel nozzle exit velocity of 11 ± 0.5 ft/sec into a subsonic airstream. Testing was conducted at free-stream flight velocities ranging from 200 to 400 knots at altitudes ranging from 12,000 to 25,000 feet. Fuel was dispersed into the subsonic airstream at fuel flow rates of approximately 13, 75, and 290 lbm/min. Holograms to record fuel droplets were taken with a ten-megawatt, pulsed ruby laser in-line holography system.

4.1 AIRSTREAM VELOCITY

The airstream velocities at the fuel injection station and the holography station were calculated from the pressures and temperatures measured at the respective stations. The variation in airstream velocity between the two stations is shown in Fig. 7.

The airstream velocity in the test volume was calculated from the total-pressure and total-temperature measurements at the holography station and the static pressure measurement in the holography system protective tubes. During one test period, end plates (Fig. 8) were installed on the end of each protective tube to evaluate their effect on airstream velocity in the test volume. The end plates failed structurally at an approach velocity of 400 knots, leaving only the plate-mounting flanges (Fig. 8) in place. The variation in the test volume airspeed with holography tube end configuration is shown in Fig. 9. With no end plates or flanges installed, the test volume airstream velocity was from 25 to 32 percent higher than the approach velocity over an approach velocity range from 200 to 480 knots. Addition of the tube end plate-mounting flanges reduced test volume airspeed by approximately 10 percent, and addition of the end plates further reduced test volume airspeed by approximately 7 to 10 percent. However, holograms of fuel droplets taken with the various tube end configurations indicated no configuration, velocity, or altitude effects on average fuel droplet size or distribution. Therefore, in the presentations to follow, the test conditions (airspeed and altitude) are those calculated at the fuel injection station.

4.2 FUEL DROPLET DATA

A summary of the test conditions and significant data is presented in Table 2. Data were obtained for all conditions tested (Table 3) except one (200-knot velocity, 12,000-ft altitude, and 290-lbm/min fuel flow rate). The low velocity and high fuel flow rate caused enough window contamination to render useless the two holograms taken at that test condition. Forty-six holograms were taken at the 15 planned test conditions, of which 36 holograms yielded useful data. A total of 1295 droplets were counted and measured. The largest droplet measured was 100 microns in diameter, and 96 percent of the droplets measured were less than 50 microns in diameter. The arithmetic average diameter of all fuel droplets measured was 27 microns, and the mass-weighted average diameter was 32 microns.

Fuel droplet size distribution histograms for representative data points, showing variations with airstream velocity, altitude, and fuel flow rate, are shown in Figs. 10, 11, and 12, respectively. The average fuel droplet size as a function of airstream velocity, altitude, fuel flow rate, fuel temperature, and nozzle injection angle is shown in Figs. 13 through 16. Average fuel droplet size was not significantly affected by any of the test variables. All data (average fuel droplet size) obtained during the program are presented in Fig. 17. All of the arithmetic average droplet diameters were within a 19- to 36-micron band with a mean value of 27.5 microns.

Since the test variables had no significant effect on the average droplet size, droplet diameter data taken at similar airstream velocities were averaged together regardless of fuel flow rate, altitude, injection angle, or fuel temperature. This produced eleven data points with statistically better averages due to a larger numerical sampling of fuel droplets. These data points were compared to previously published data (Refs. 5, 6, and 7) in Figs. 18 and 19 as a function of ΔV.

4.3 COMPARISON WITH PREVIOUSLY PUBLISHED RESULTS

In Fig. 18, the JP-4 test data obtained during this test program are compared to the results obtained in Ref. 5, in which a similar test installation configuration and holography system were used to determine droplet sizes and size distribution of a simulated defoliant fluid dispersed into a subsonic airstream. Maximum droplet diameter measured was 50 microns. The data of Ref. 5 substantiate the level of the data from the JP-4 fuel droplet test within the uncertainty level of the data.

In Ref. 6, Nukiyama and Tanasawa present the empirical equation

$$d_o = \frac{585}{\Delta V} \left(\frac{\sigma}{\rho}\right)^{1/2} + 597 \left(\frac{\mu}{\sqrt{\rho\sigma}}\right)^{0.45} (1000 \; Q_\ell/Q_a)^{1.5} \qquad (4.1)$$

where ΔV is in m/sec and the other variables are in the cgs systems of units. This empirical equation was obtained from test data for a solution of water, alcholol, and glycerine. The solution composition was varied in order to vary the density, surface tension, and/or viscosity as desired.

Nukiyama and Tanasawa (Ref. 6) found that, for larger values of volumetric flow ratio, $Q_a/Q\ell$, the effects of liquid viscosity and $Q_a/Q\ell$ on the liquid droplet size become small. For water, the effects of liquid viscosity and $Q_a/Q\ell$ on droplet size become negligible when $Q_a/Q\ell$ exceeds 5000. The test installation used for the JP-4 fuel tests was significantly different from that of Ref. 6, primarily because the airflow from the test cell "nozzle" was contained by test section walls in the JP-4 fuel tests. It is not certain that the parameter $Q_a/Q\ell$ can be applied to the JP-4 fuel test. However, the ratio of test cell volumetric airflow rate to volumetric fuel flow rate was in excess of 25,000. For purposes of verifying the level of the JP-4 fuel droplet data, it was assumed that the second term of Eq. (4.1) would have a small effect, if any, and the Nukiyama-Tanasawa equation could be reduced to

$$d_o = \frac{585}{\Delta V} \left(\frac{\sigma}{\rho} \right)^{\frac{1}{2}} \tag{4.2}$$

Average JP-4 droplet diameter, calculated from the above simplified equation, is shown in Fig. 18.

The mass-weighted average JP-4 droplet diameter is presented in Fig. 19 as a function of ΔV and is compared to the test data reported in Ref. 7. The results of Ref. 7 (Fig. 19) are for water, isooctane, and benzene injected transversely into airstreams with ΔV of 207 and 414 knots. Maximum droplet diameters were 125 microns (for benzene) at 207-knots airstream velocity and 75 microns (for water) at 414 knots. Although the method of injection (transverse) is not the same as that employed for this test program (axial), the average droplet sizes produced are comparable as shown in Ref. 6. Data from Refs. 6 and 7 support the conclusion of this program that liquid injection angle has negligible effect on droplet size. It should be noted, however, that this conclusion is valid only when proper injection nozzle design is employed so that airstream eddies downstream of the nozzle are minimized. The conclusion that liquid temperature has little effect on droplet size is also supported by Ref. 7, in which almost identical average droplet sizes were obtained for liquid temperatures ranging from 98 to 200°F.

Ingebo and Foster (Ref. 7) indicate that mass-weighted average droplet diameter is proportional to the square root of the nozzle inside diameter. Nukiyama and Tanasawa (Ref. 6) found that, within the limits of the variation of test parameters employed, the liquid injection nozzle shape and size (three nozzles, from 0.25- to 0.76-mm ID) have

11

no effect on average droplet size. Davidson's results (Ref. 5) (six nozzles, from 0.152- to 1.079-in. ID) and the results of this test program (four nozzles, from 0.260- to 1.41-in ID) verify that nozzle size does not affect droplet size.

Nukiyama and Tanasawa (Ref. 6) concluded that, for a given liquid, large values of Q_a/Q_ℓ and constant air density, the governing parameter for average droplet size, is the velocity difference between the air and the liquid. Ingebo and Foster (Ref. 7) showed that the mass-weighted average droplet diameter was inversely proportional to the 3/4 power of the airstream velocity. The test data of this program do not reflect any significant effect of velocity. However, over the velocity range of interest, the 15-micron decrease in average droplet diameter indicated in Refs. 6 and 7 is within the data uncertainty band of ±9.5 microns for the JP-4 fuel data.

5.0 SUMMARY OF RESULTS

Test program objectives were to determine the size and distribution of fuel droplets as a function of flight velocity, altitude, fuel flow rate, fuel temperature, and fuel nozzle injection angle when fuel was dispersed at a constant fuel nozzle exit velocity of 11 ± 0.5 ft/sec into a subsonic airstream. Testing was conducted at free-stream flight velocities ranging from 200 to 400 knots at altitudes ranging from 12,000 to 25,000 feet. Fuel was dispersed into the subsonic airstream at fuel flow rates of approximately 13, 75, and 290 lbm/min. Holograms to record fuel droplets were taken with a ten-megawatt, pulsed ruby laser in-line holography system.

The results of the program are summarized as follows:

1. Average fuel droplet diameter was not significantly affected by any of the test variables.

2. The arithmetic average diameter of all fuel droplets measured was 27 microns, and the mass-weighted average diameter was 32 microns.

3. The largest droplet measured was 100 microns in diameter, and 96 percent of the fuel droplets measured were less than 50 microns in diameter.

4. Forty-six holograms were made at the planned test conditions, of which thirty-six yielded useful data; a total of 1295 droplets were counted and measured.

REFERENCES

1. Research Facilities Handbook., Arnold Engineering Development Center, June 1970.

2. Trolinger, J. D. and Belz, R. A. "Holography in Dust Erosion Facilities." AEDC-TR-73-160 (AD766420) September 1973.

3. Owens, C. L. "Capabilities of the ESF Instrument Branch." AEDC-TR-67-18 (AD648707) March 1967.

4. CPIA No. 180 "ICRPG Handbook for Estimating the Uncertainty in Measurements Made with Liquid Propellant Rocket Engine Systems." AD855130, April 30, 1969.

5. Davidson, D. L. "Holographic Determination of the Droplet Size Distribution of a Simulated Defoliant Spray in a 400-Knot Airstream." AEDC-TR-70-137, AFATL-TR-70-47 (AD880066), May 1970.

6. Nukiyama, Shirō and Tanasawa, Yasushi. "Experiments of the Atomization of Liquids in an Air Stream." Defence Research Board, Department of National Defence, Ottawa, Canada, March 19, 1950 (Translated from Transactions of the Society of Mechanical Engineers (Japan), Vols. 4, 5 and 6, 1938-1940 by E. Hope).

7. Ingebo, Robert D. and Foster, Hampton, H. "Drop-size Distribution for Crosscurrent Breakup of Liquid Jets in Airstream." NACA TN 4087, October 1957.
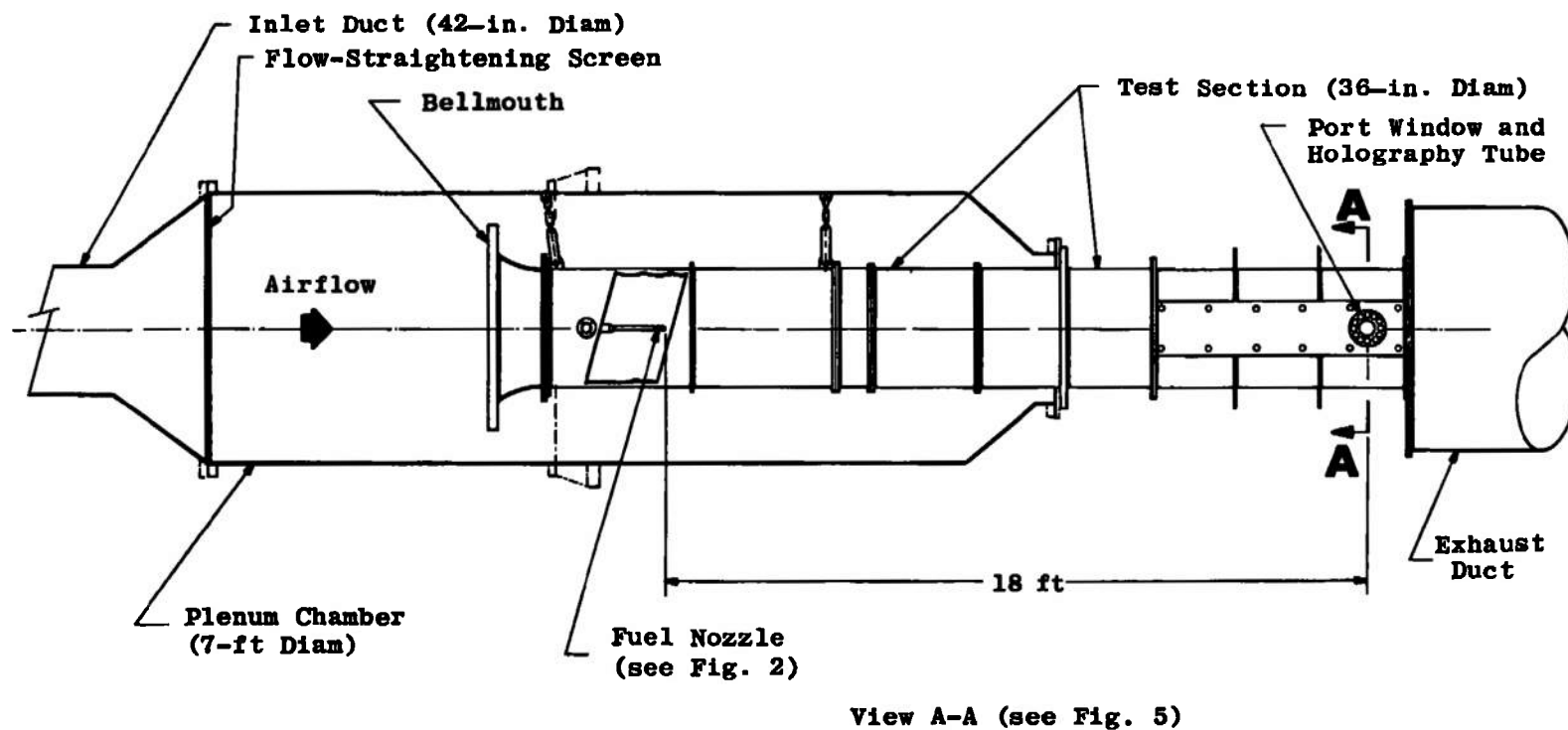
Figure 1. JP-4 fuel dump test installation in Propulsion Research Cell (R-2B).

a. Three straight nozzles

a	b	c
0.260	0.50	0.60
0.652	0.75	0.85
1.320	1.54	1.54
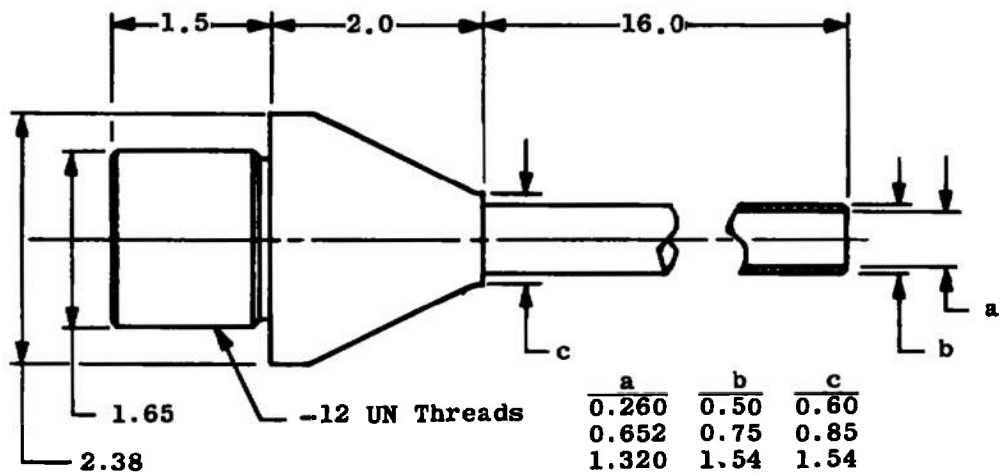
All Dimensions in Inches
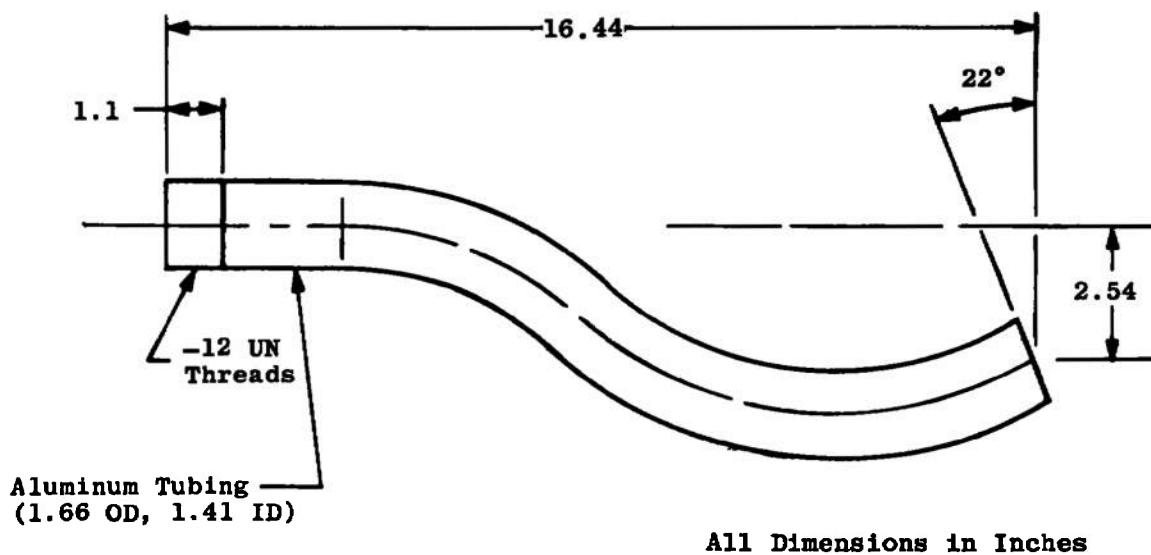
b. Canted nozzle

Figure 2. Schematic of fuel nozzles.
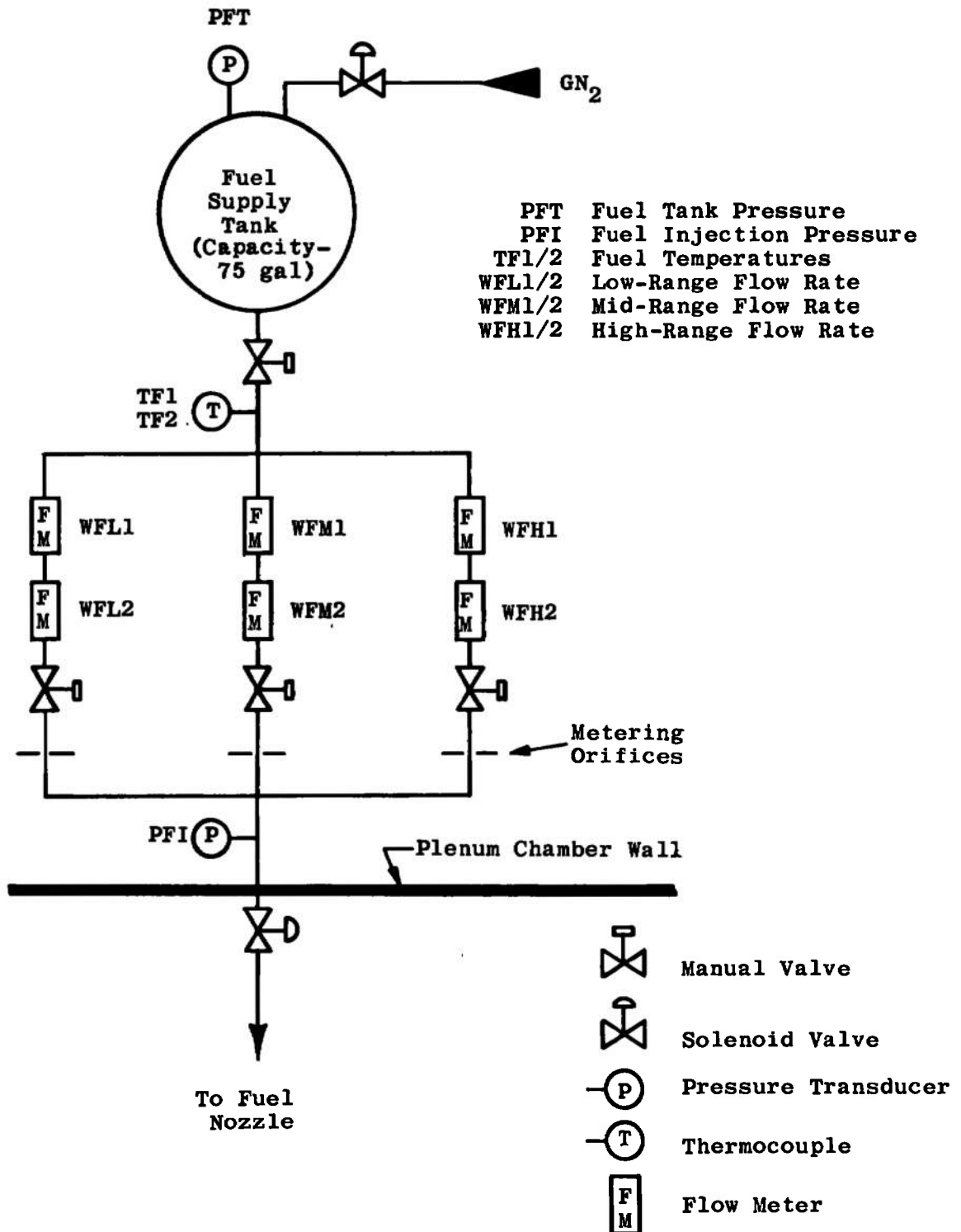
Figure 3. Fuel system schematic.

Test Volume
(2.0 Diam,
1.0 Length)

2.0 Optical Stop
(Collimating Lens)

Imaging
Lens
$f\ell$=19.5
F4.5

Microscopic Objective
and Spatial Filter

Film
Pack

Q-Switch

Quartz Windows
(6.0 Diam,
1.0 Thick)

1.0

Ruby
Rod

Protective Tubes
(3.0 ID, 3.5 OD)

Movable Mirrors

Test Section
(36.66 Diam)

He/Ne Alignment Laser

All Dimensions in Inches

18
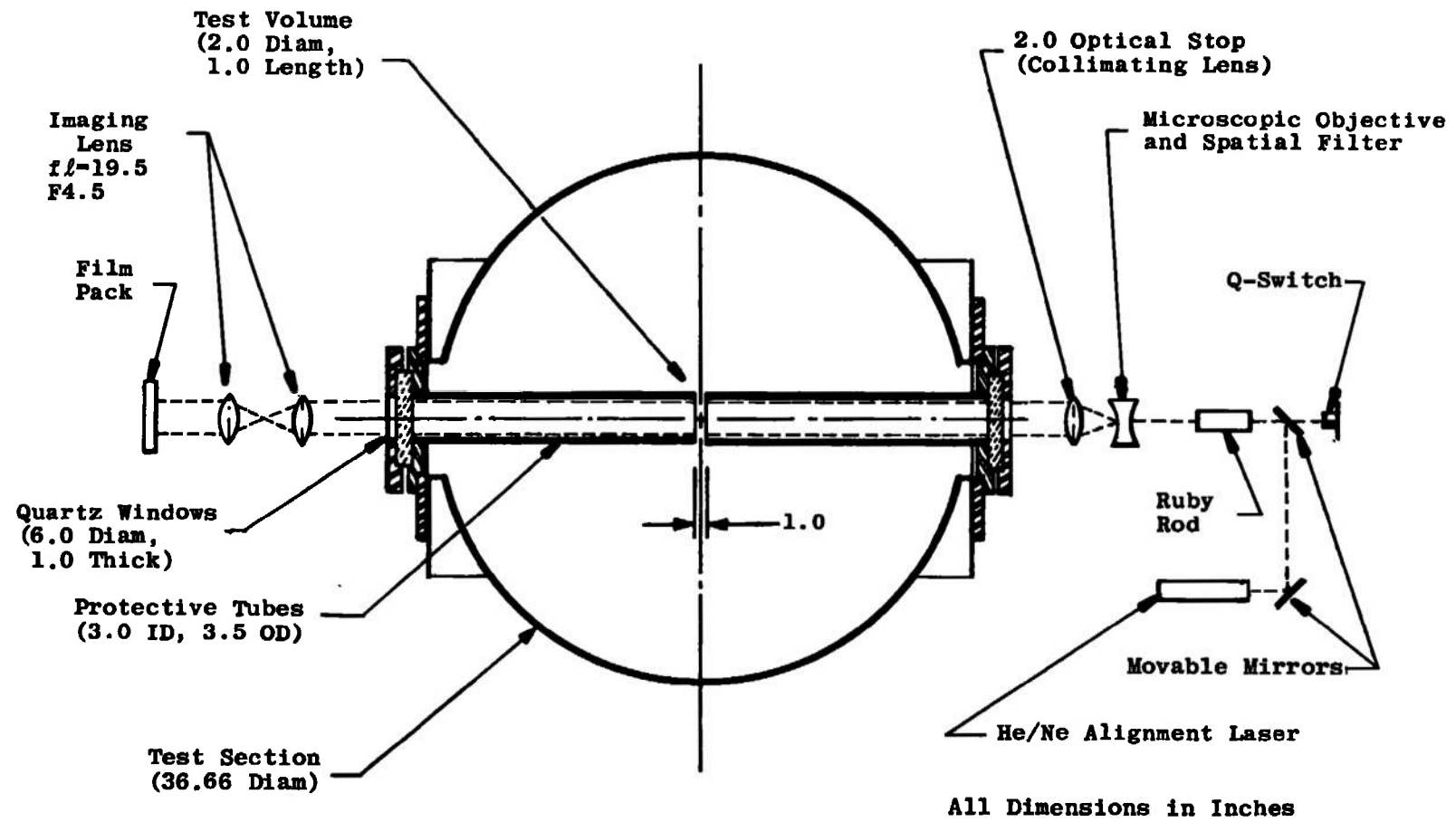
Figure 4. Schematic of holography system.
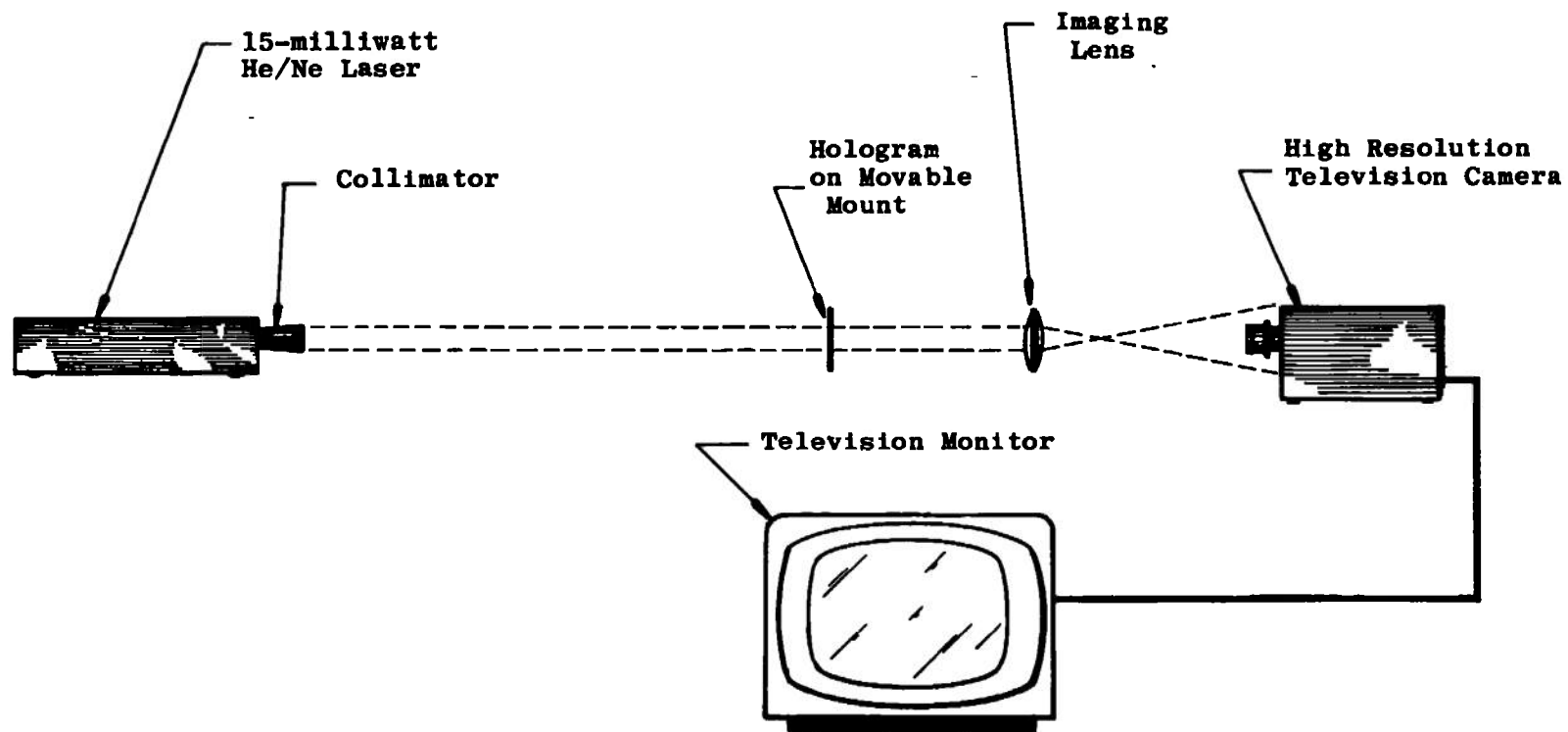
Figure 5. Schematic of hologram reconstruction technique.

Fuel
Injection
Station
A

Holography
Station

H

Airflow

18 ft
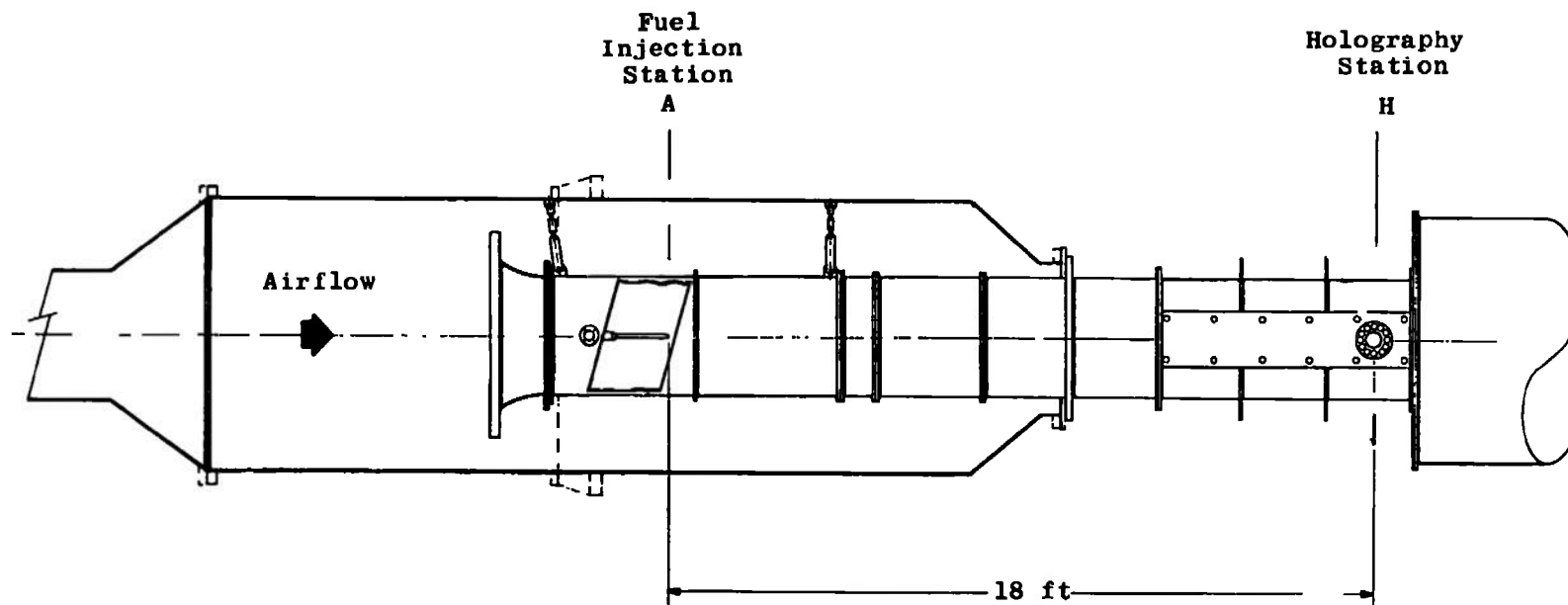
Station Parameter	A	H
Wall Static Pressure	4	2
Total Pressure	4	4
Total Temperature	2	2

a. Station locations
Figure 6. Aerodynamic instrumentation schematic.

Station A

Fuel Injection Station

● Static Pressure
O Total Pressure
X Total Temperature

All Dimensions in Inches

Station H

Holography Station (18 ft Downstream of Station A)
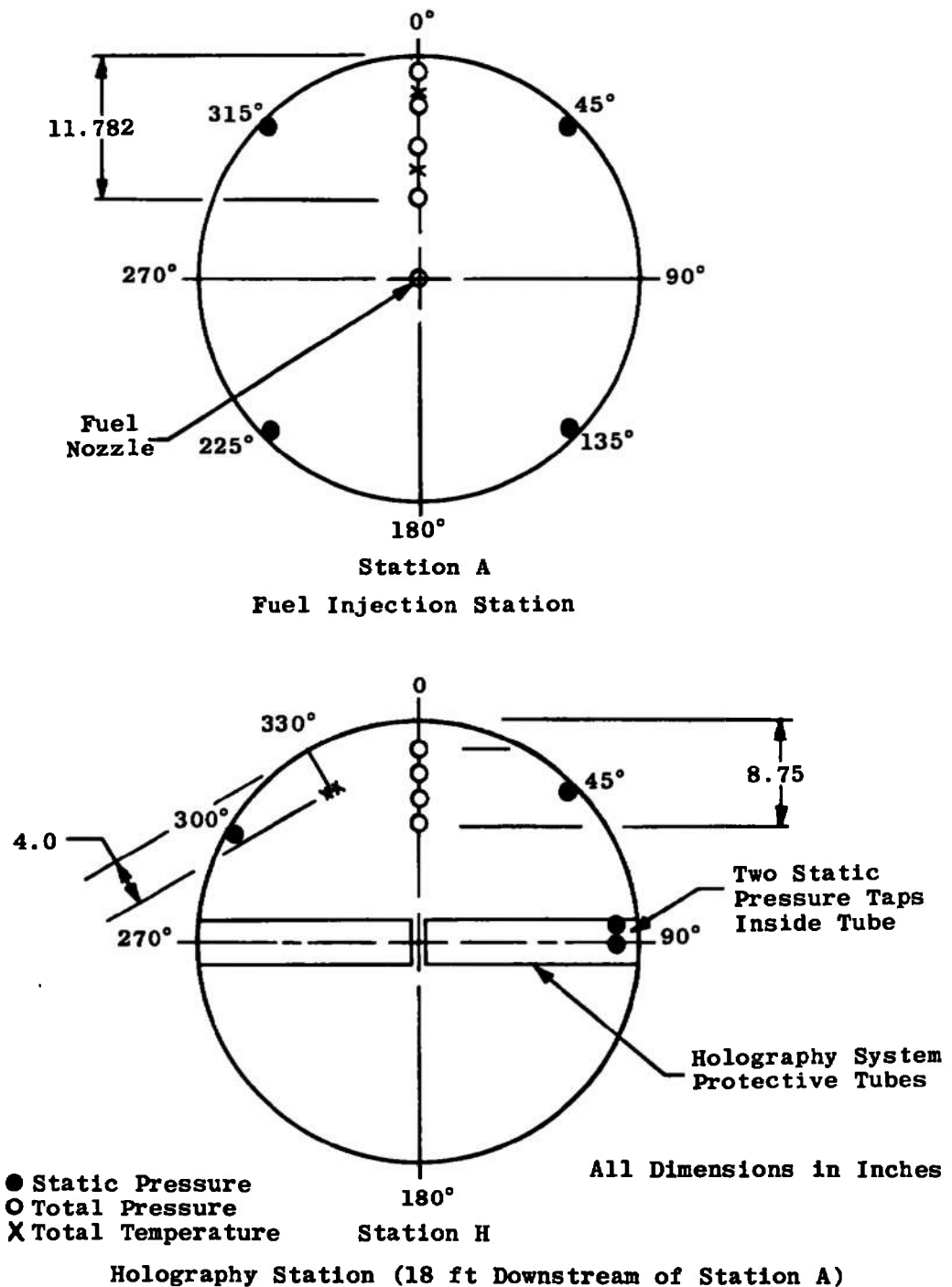
b. Instrumentation details (looking upstream)
Figure 6. Concluded.

21
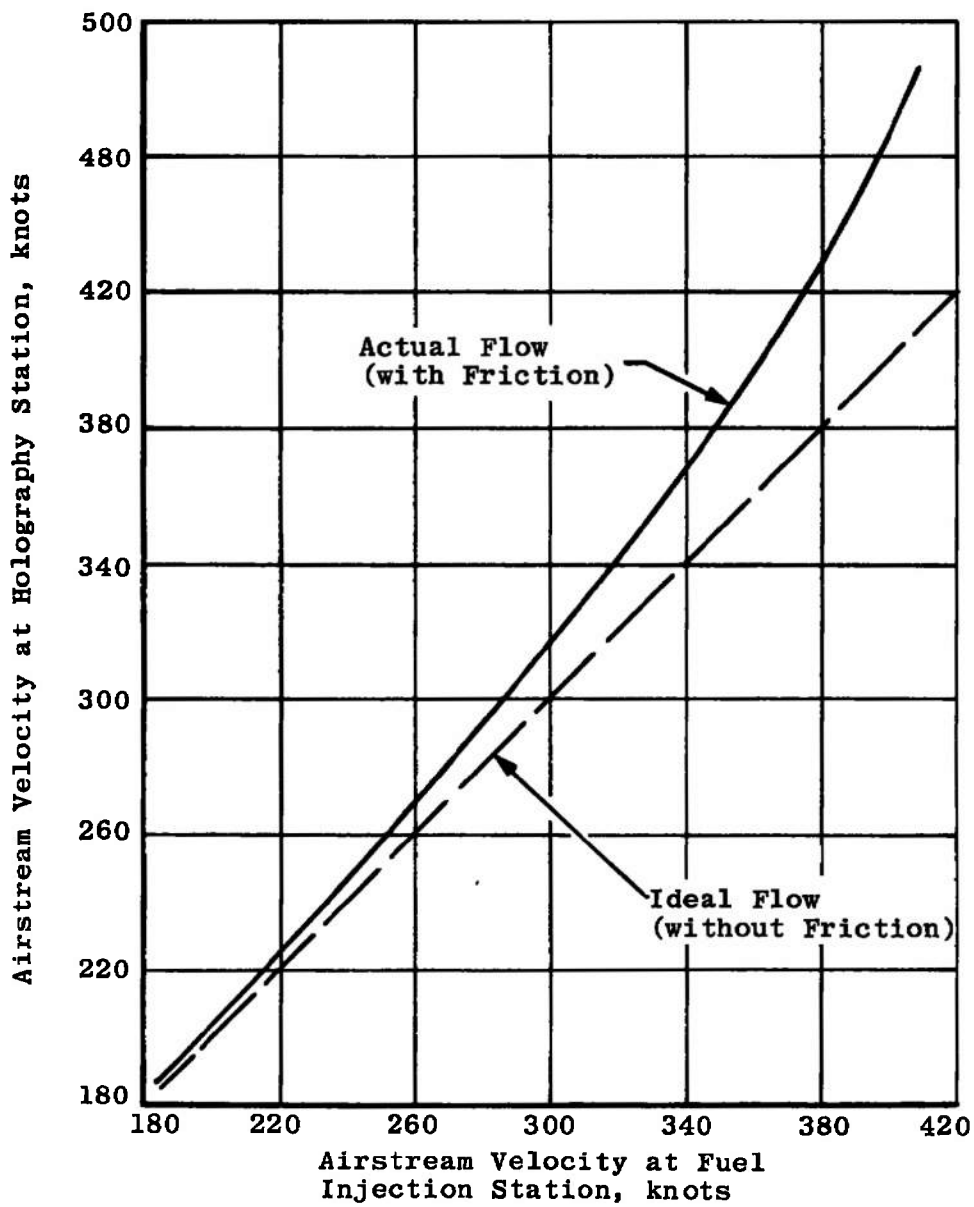
Figure 7. Comparison of airstream velocities at fuel injection
station and holography station.

Test
—⊄— Airflow
Section

Mounting Flange
(6.75 Diam)

Holography System
Protective Tube

0.5

End Plate
(0.125 Thick)

Collar
(3.50 ID, 3.75 OD)

All Dimensions in Inches

12.0

4.5

End Plate
Mounting Flange
Collar

Airflow

7.5

15.0

Sharp Edge
(15° Bevel)
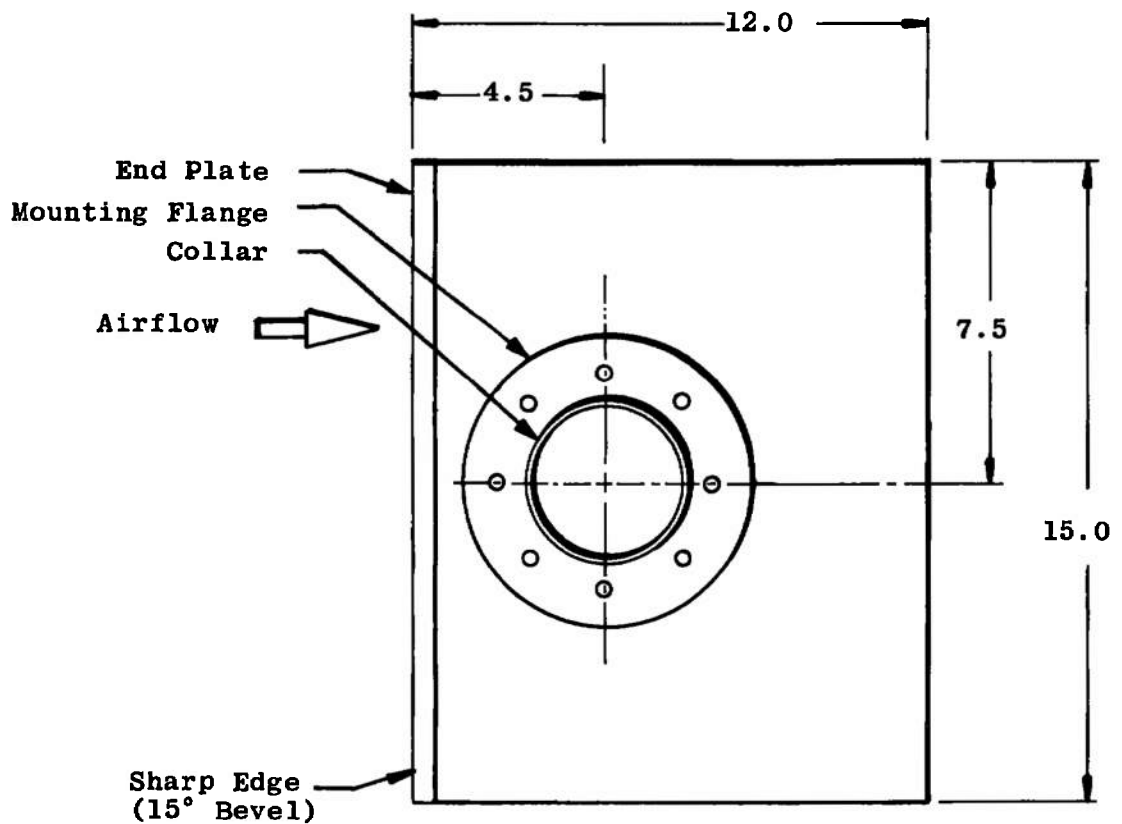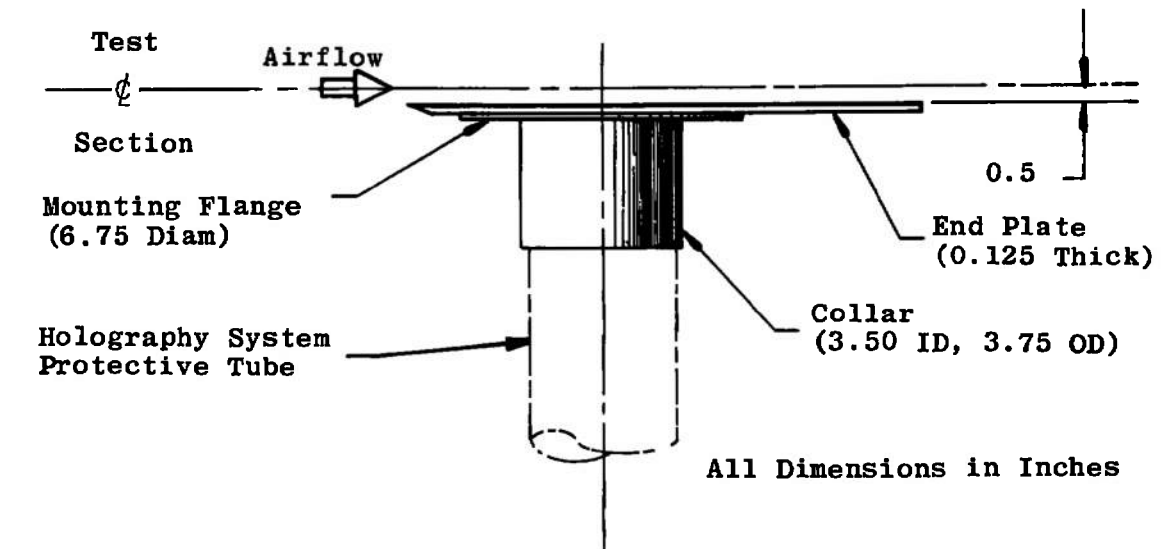
Figure 8. Schematic of holography system protective tube end plates.
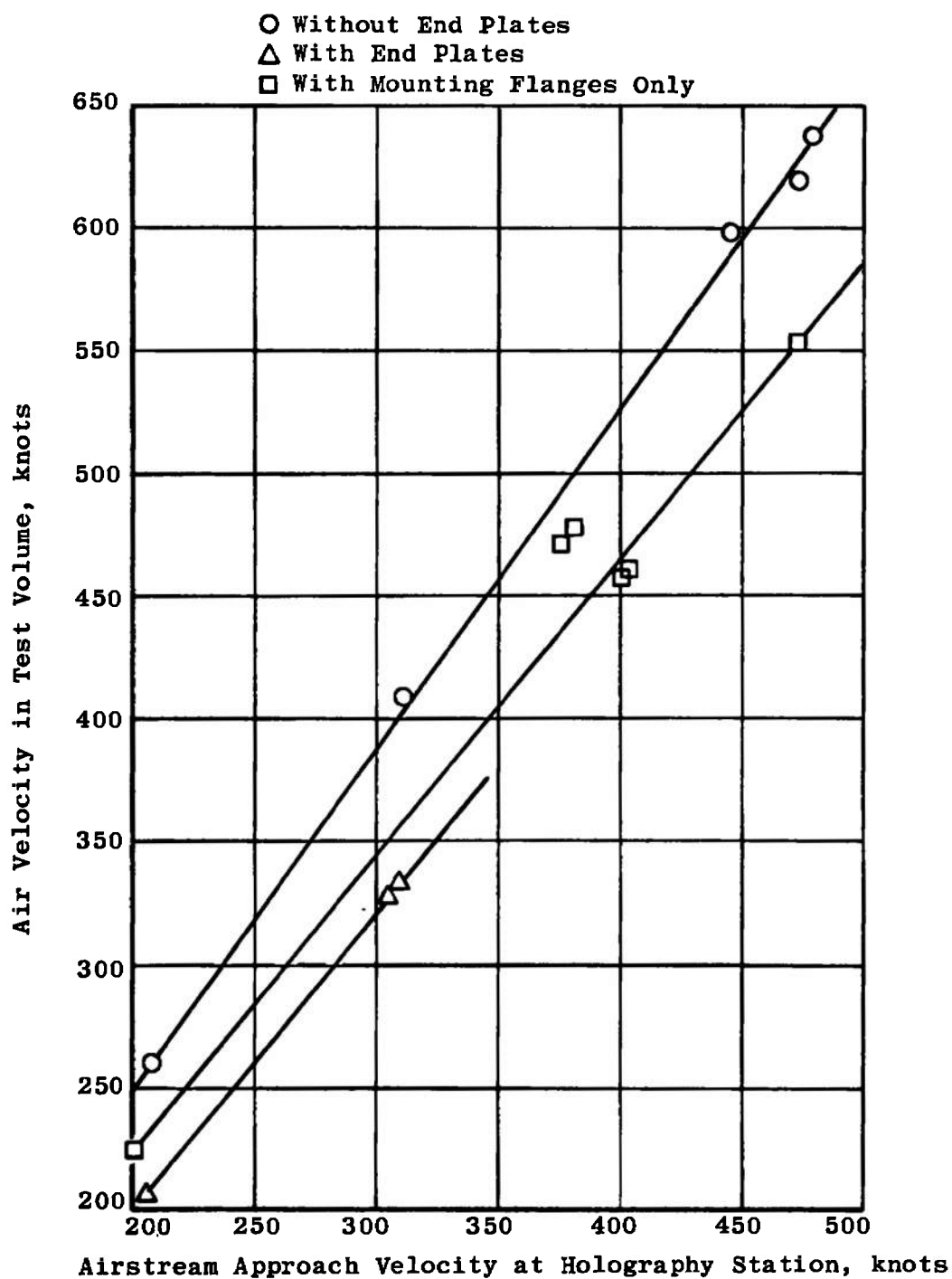
Figure 9. Airstream velocity in the holography test volume as a function of airstream approach velocity at the holography station.

$\overline{d} = 27$ microns

$\overline{d}_m = 31$ microns

$$\Psi = \frac{n]_{d_1}^{d_2}}{n_t} \text{ , Relative Frequency of Occurrence}$$

Droplet Diameter, microns

a. Airstream velocity = 214 knots

$\overline{d} = 23$ microns

$\overline{d}_m = 28$ microns

Droplet Diameter, microns

b. Airstream velocity = 313 knots

$\overline{d} = 35$ microns

$\overline{d}_m = 39$ microns

Droplet Diameter, microns

c. Airstream velocity = 387 knots
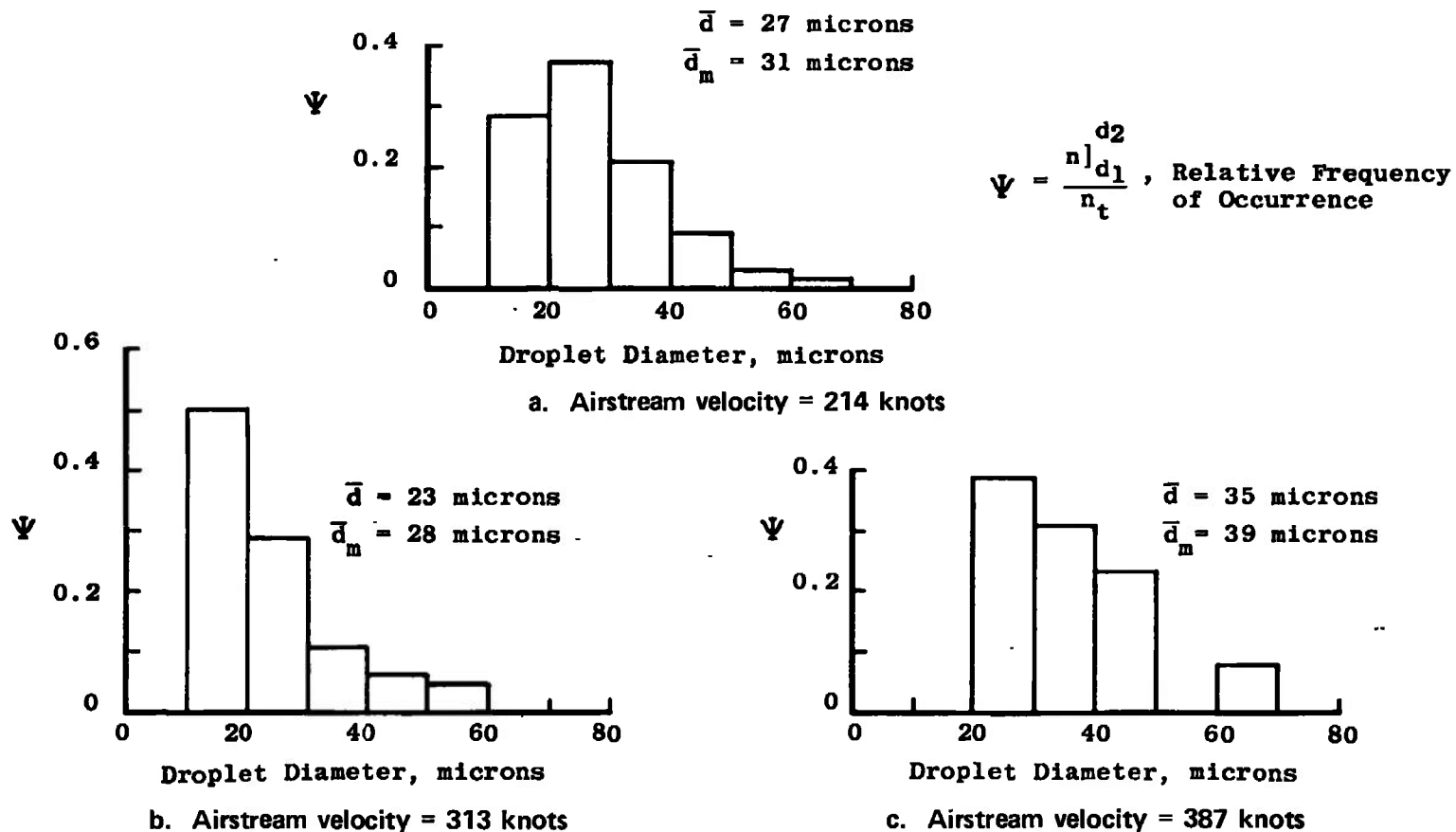
Figure 10. Typical histograms of fuel droplet size distributions, variation with fuel injection
station airstream velocity (12,000-ft altitude, 13-lbm/min fuel flow rate).
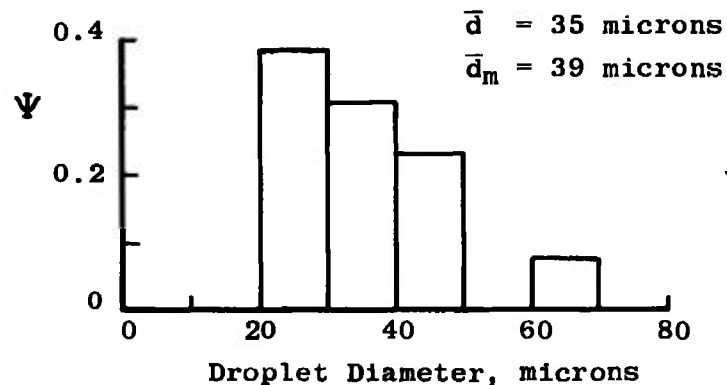
$$\Psi = \frac{n]_{d_1}^{d_2}}{n_t} \text{, Relative Frequency of Occurrence}$$

$\overline{d}$ = 35 microns

$\overline{d}_m$ = 39 microns

a. Altitude = 12,100 ft

$\overline{d}$ = 25 microns

$\overline{d}_m$ = 28 microns

b. Altitude = 19,500 ft

$\overline{d}$ = 27 microns

$\overline{d}_m$ = 31 microns
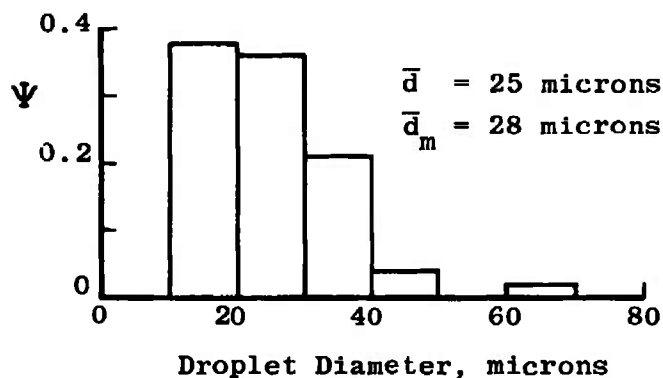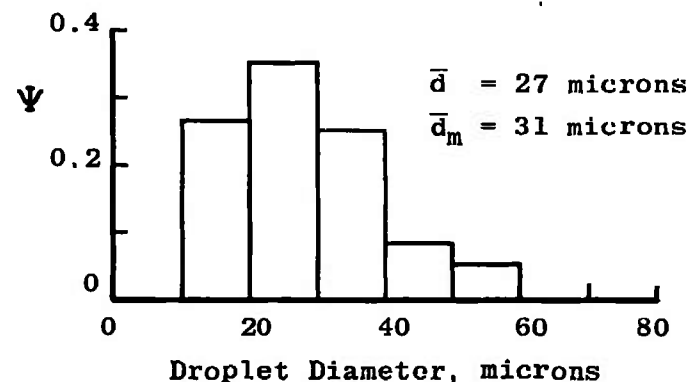
c. Altitude = 24,800 ft

Figure 11. Typical histograms of fuel droplet size distributions, variation with fuel injection station altitude (400-knot airstream velocity, 13-lbm/min fuel flow rate.

$$\Psi = \frac{n]_{d_1}^{d_2}}{n_t} \text{ , Relative Frequency of Occurrence}$$

$\overline{d}$ = 23 microns

$\overline{d}_m$ = 28 microns
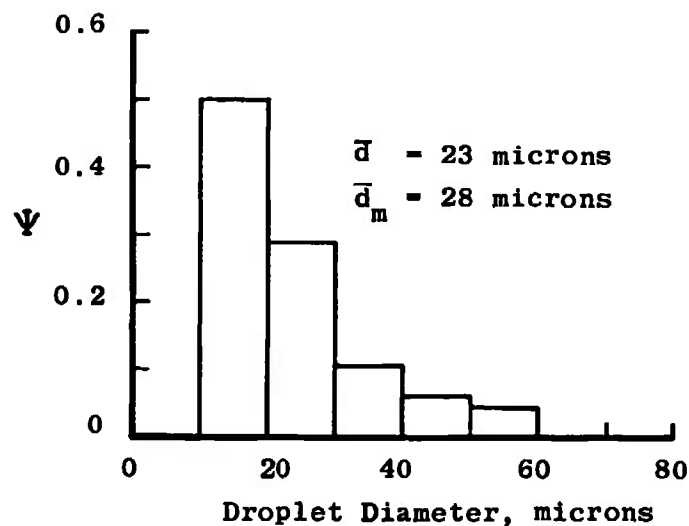
a. Fuel flow rate = 13 lbm/min

$\overline{d}$ = 31 microns

$\overline{d}_m$ = 33 microns
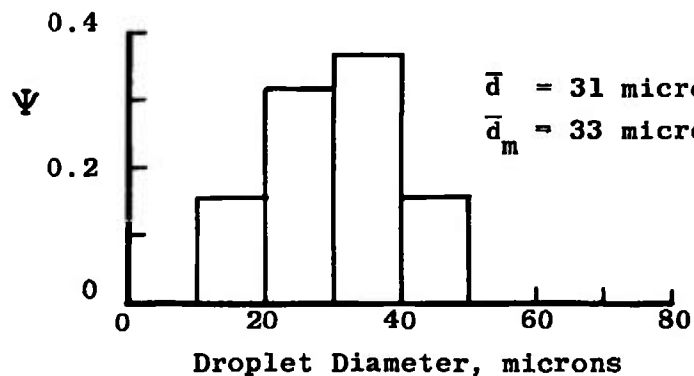
b. Fuel flow rate = 75 lbm/min

$\overline{d}$ = 27 microns

$\overline{d}_m$ = 33 microns
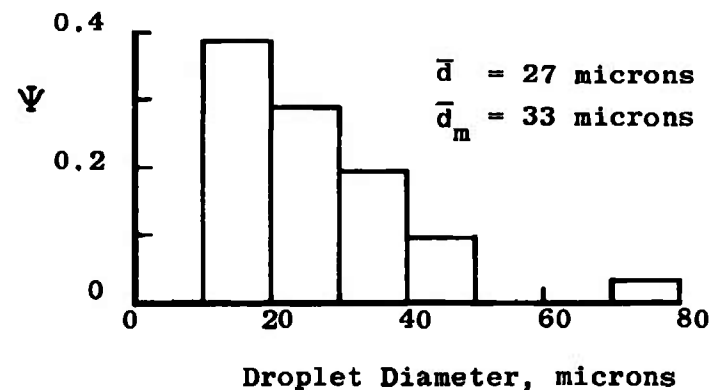
c. Fuel flow rate = 289 lbm/min

Figure 12. Typical histograms of fuel droplet size distributions, variation with fuel flow rate (300-knot airstream velocity, 12,000-ft altitude).
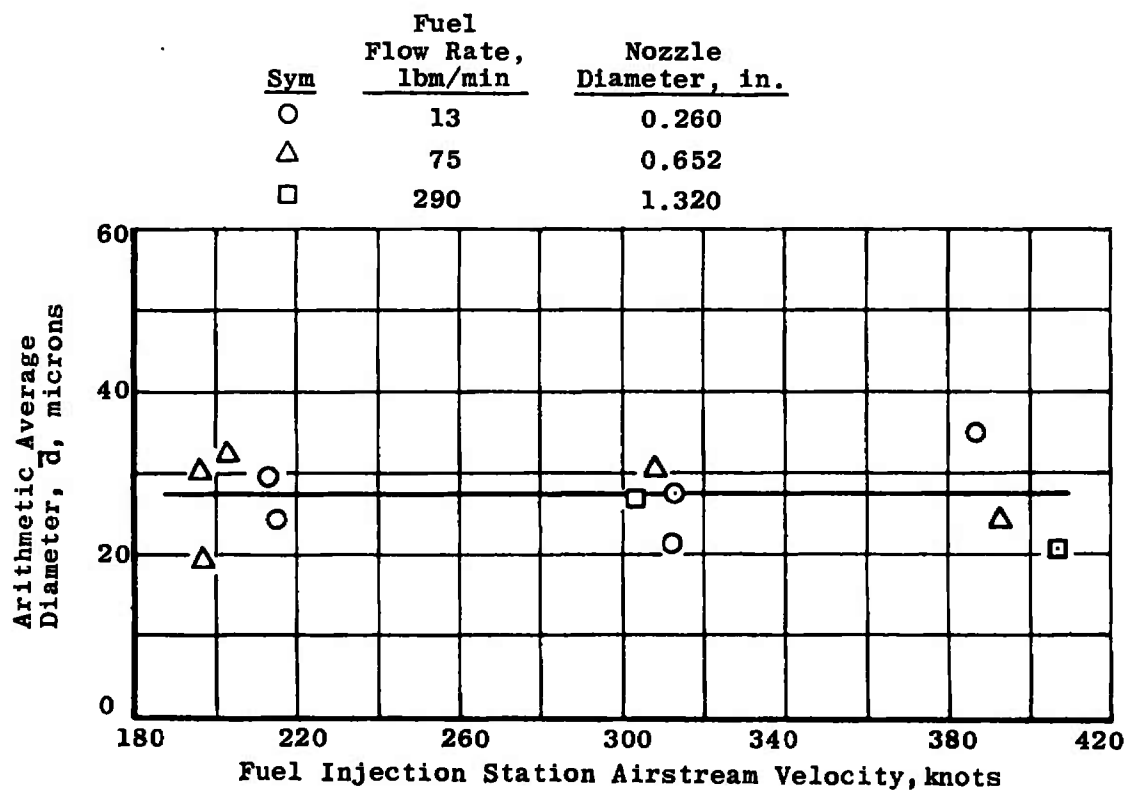
Sym	Fuel Flow Rate, lbm/min	Nozzle Diameter, in.
O	13	0.260
△	75	0.652
□	290	1.320

a. Arithmetic average fuel droplet diameter
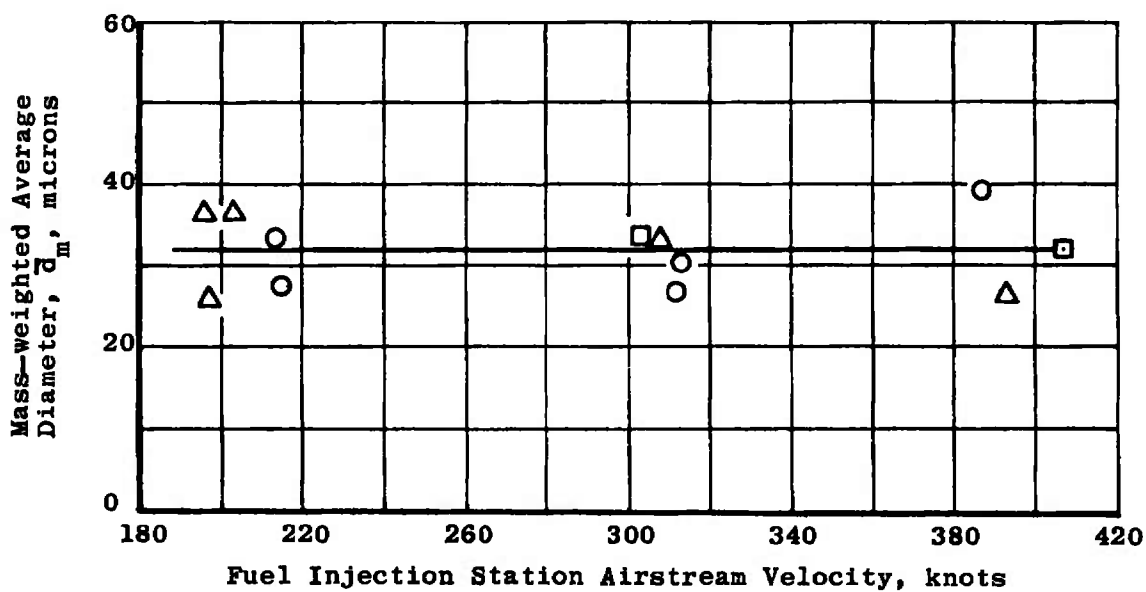
b. Mass-weighted average fuel droplet diameter

Figure 13. Variation of fuel droplet average diameters with airstream velocity at 12,000-ft altitude (straight nozzles).
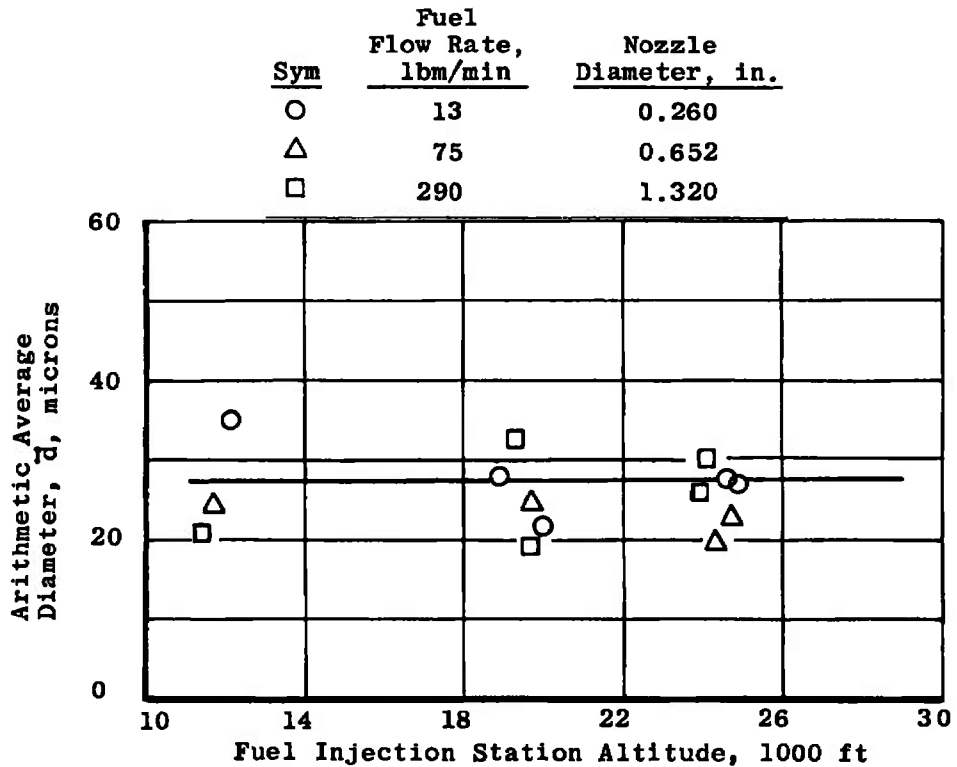
28

Sym	Fuel Flow Rate, lbm/min	Nozzle Diameter, in.
O	13	0.260
△	75	0.652
□	290	1.320

a. Arithmetic average fuel droplet diameter
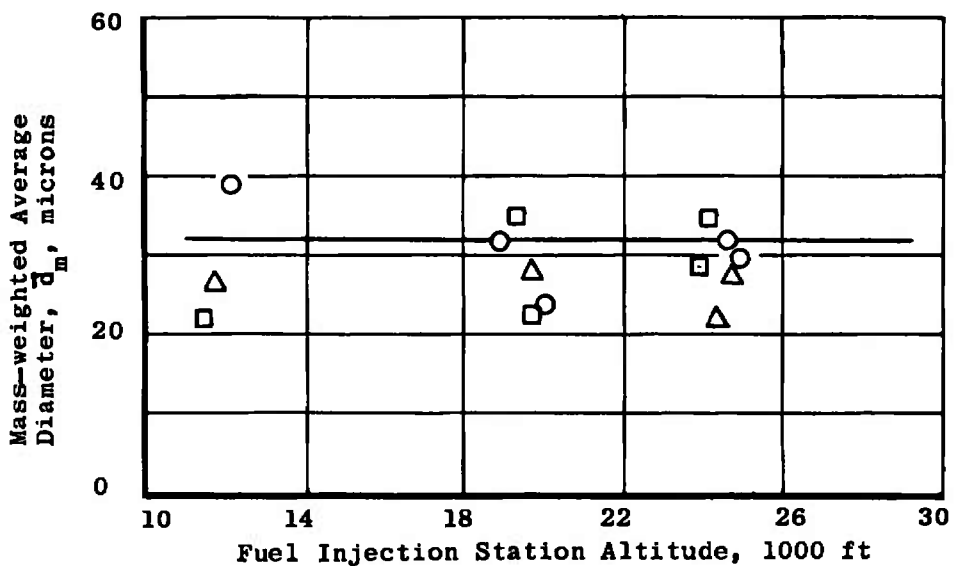
b. Mass-weighted average fuel droplet diameter

Figure 14. Variation of fuel droplet average diameters with altitude at fuel injection station airstream velocity of 400 knots (straight nozzles).

Sym	Fuel Temperature, °F	Fuel Flow Rate, lbm/min	Nozzle, in., ID
O	67	13	0.260 Straight
●	29 to 48	13	0.260 Straight
□	72	290	1.32 Straight
■	21, 33	290	1.32 Straight
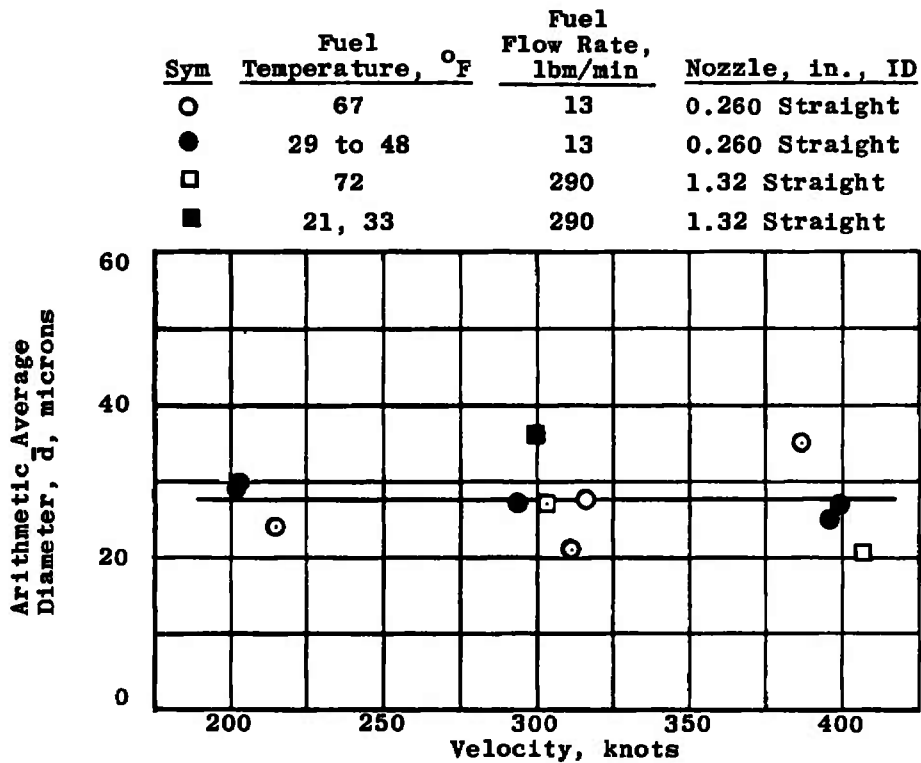
a. Variation with fuel injection station airstream velocity (altitude of 12,000 ft)
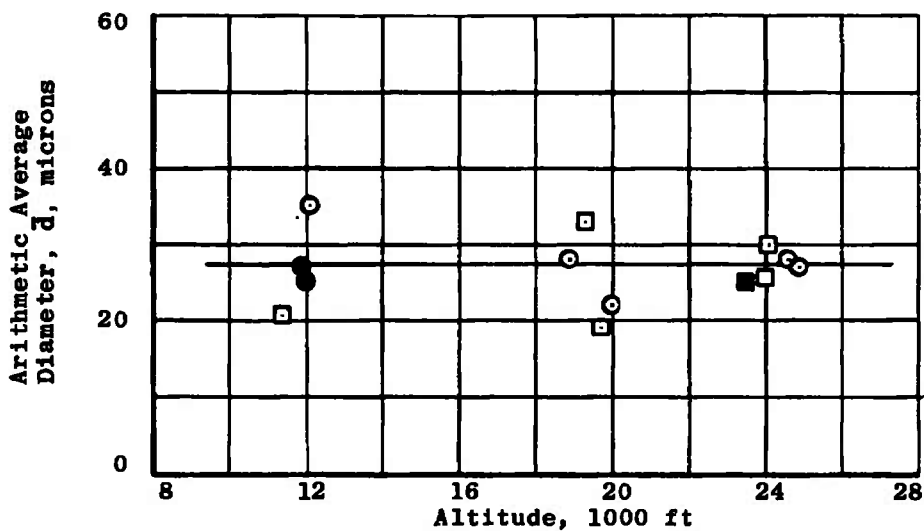
b. Variation with fuel injection station altitude (velocity of 400 knots)

Figure 15. Variation of arithmetic average fuel droplet diameter with velocity and altitude showing effect of fuel temperature.
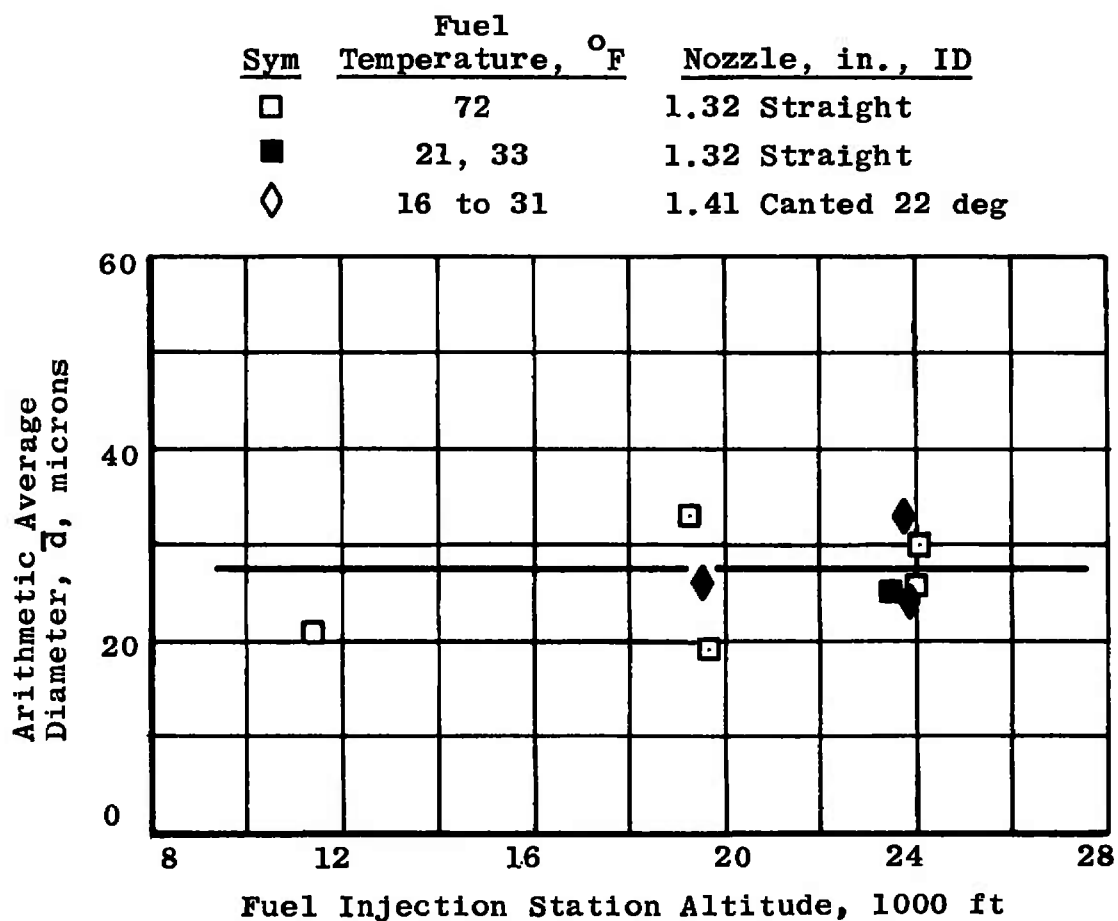
Figure 16. Variation of arithmetic average fuel droplet diameter with
altitude showing effect of nozzle injection angle (fuel flow
rate of 290 lbm/min).
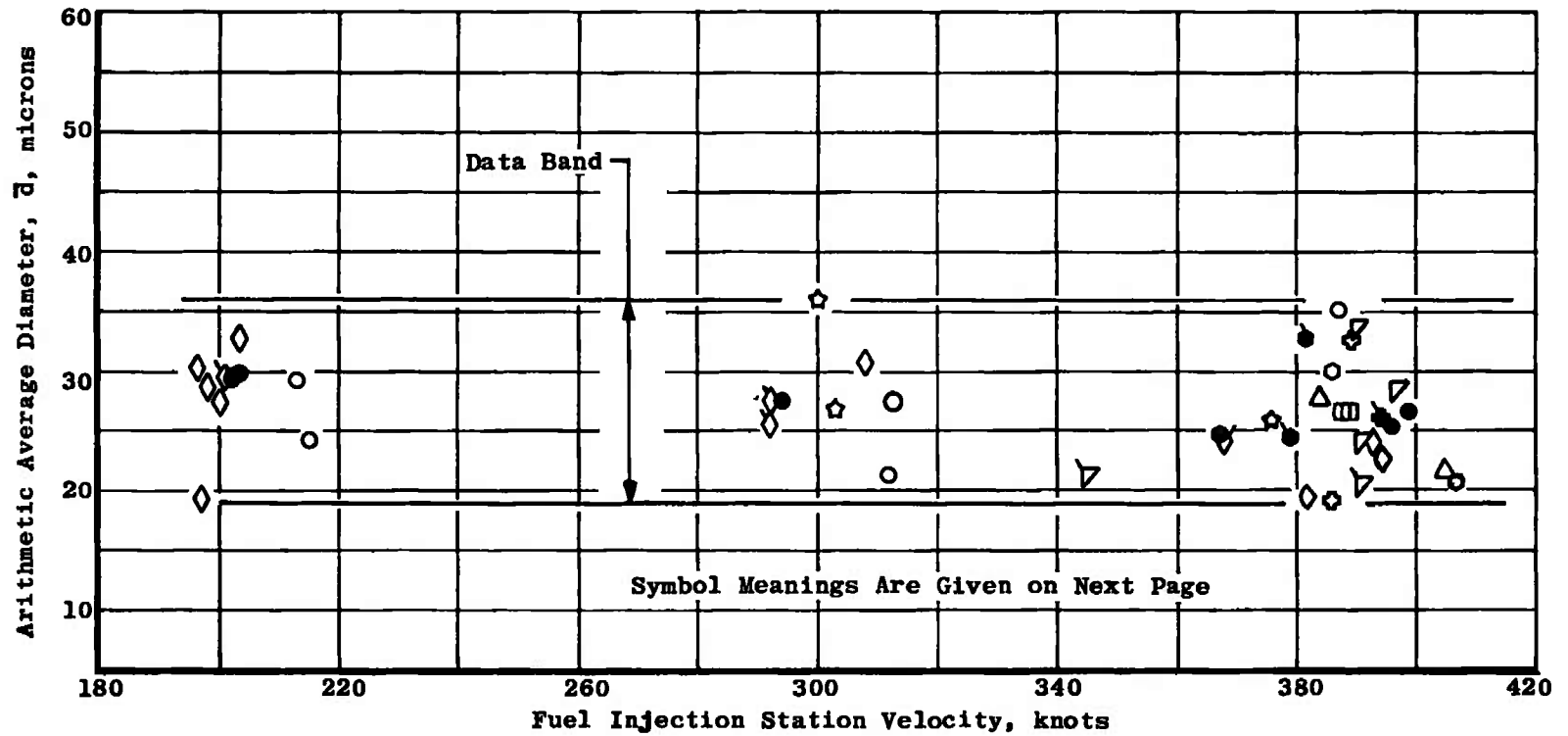
Figure 17. Arithmetic average fuel droplet diameter versus fuel injection station airstream
velocity for all configurations and test conditions.

Symbol	Fuel Flow Rate, lbm/min	Altitude, 1000 ft	Nozzle Diameter (in.) and Configuration	Fuel Temperature, °F
○	13	12	0.260 Straight	67
●	13	12	0.260 Straight	29—48
△	13	20	0.260 Straight	67
□	13	24	0.260 Straight	67
◊ *	75	12	0.652 Straight	67
◊	75	12	0.652 Straight	67
▽ *	75	20	0.652 Straight	67
▽	75	20	0.652 Straight	67
◊	75	24	0.652 Straight	67
⬠	290	12	1.320 Straight	73
⬟	290	12	1.320 Straight	33
⬢	290	20	1.320 Straight	73
⬢	290	20	1.410 Canted	31
○	290	24	1.320 Straight	72
●	290	24	1.320 Straight	21
⬢	290	24	1.410 Canted	16,19

*End Plates Installed on Holography System Protective Tubes

Symbols for Figure 17
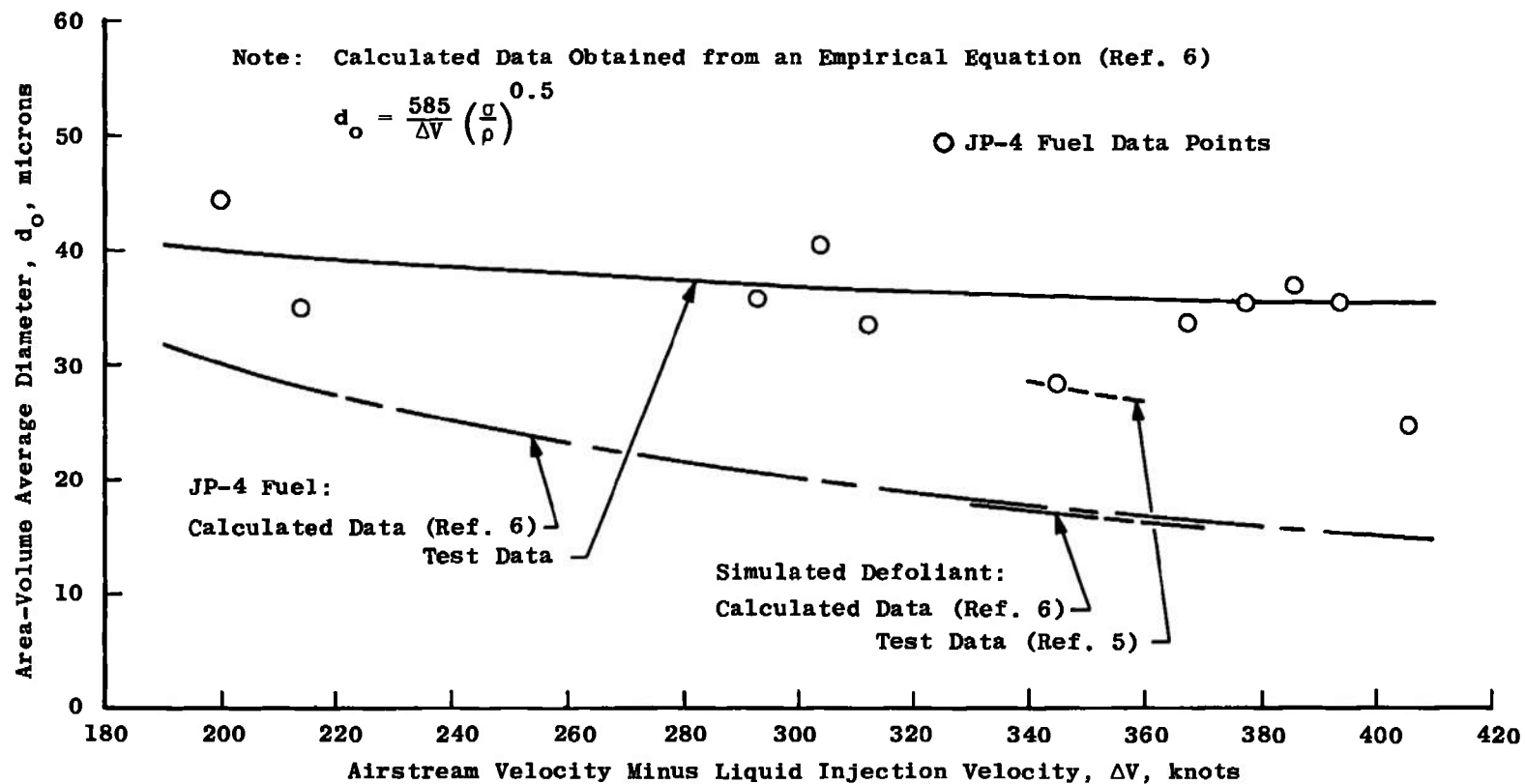
Figure 18. Comparison of area-volume average droplet diameter data with previously published results.
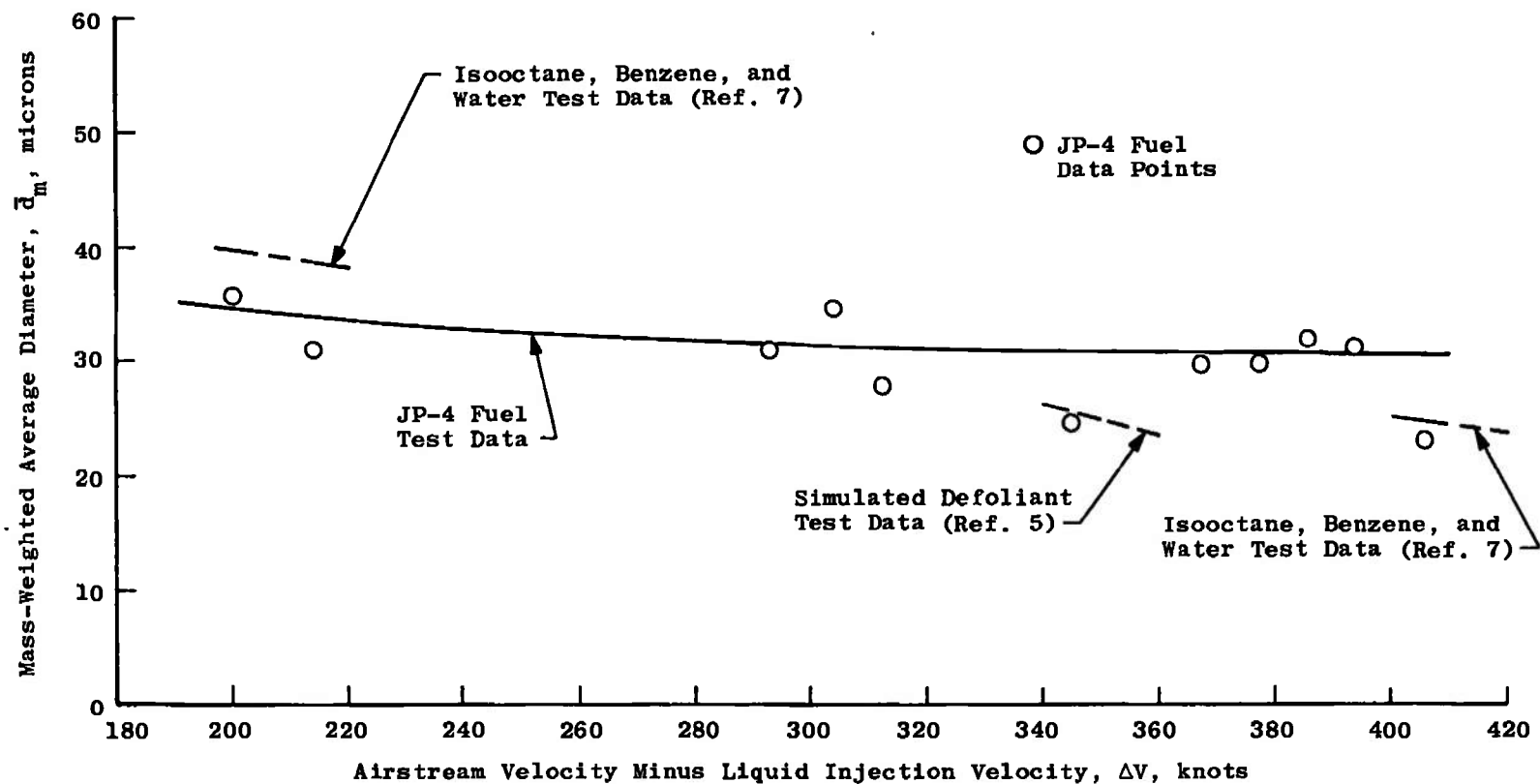
Figure 19. Comparison of mass-weighted average droplet diameter data with previously published results.

Table 1. Data Uncertainty

Parameter Designation	STEADY-STATE ESTIMATED MEASUREMENT[a]							Range	Type of Measuring Device	Type of Recording Device	Method of System Calibration
	Precision Index (S)			Bias (B)		Uncertainty ±(B + t₉₅S)					
	Percent of Reading	Unit of Measurement	Degree of Freedom	Percent of Reading	Unit of Measurement	Percent of Reading	Unit of Measurement				
Test Section Total, PTT1--PTT4, PSIA	±0.11	----	31	±0.21	----	±0.43	----	7 to 13 psia	Bonded Strain-Gage-Type Pressure Transducers	Sequential Sampling, Millivolt-to-Digital Converter, and Magnetic Tape Storage Data Acquisition System	Resistance Shunt Based on the Standards Laboratory Determination of Transducer Applied Pressure versus Resistance Shunt Equivalent Pressure Relationship
Test Section Static, PST1--PST4, PSIA	±0.11	----	31	±0.21	----	±0.43	----	5 to 10 psia			
Duct Wall Static, PSD1--PSD4, PSIA	±0.11	----	31	±0.21	----	±0.43	----	5 to 10 psia			
Holography Station Total, PTH1--PTH4, PSIA	±0.11	----	31	±0.21	----	±0.43	----	6 to 13 psia			
Holography Station Static, PSH1--PSH2, PSIA	±0.11	----	31	±0.21	----	±0.43	----	4 to 10 psia			
Plenum Total PTP, PSIA	±0.11	----	31	±0.21	----	±0.43	----	6 to 13 psia			
Fuel Tank PFT, PSIA	±0.11	----	31	±0.21	----	±0.43	----	30 to 160 psia			
Fuel Injection PFI, PSIA	±0.11	----	31	±0.21	----	±0.43	----	5 to 26 psia			
Holography Pipe, PHP1--PHP2, PSIA	±0.11	----	31	±0.21	----	±0.43	----	3 to 10 psia			
End Plate Static, PEP1--PEP2, PSIA	±0.11	----	31	±0.21	----	±0.43	----	3 to 10 psia			

[a]Ref. 4

Table 1. Concluded

37

Parameter Designation	STEADY-STATE ESTIMATED MEASUREMENT*							Range	Type of Measuring Device	Type of Recording Device	Method of System Calibration
	Precision Index (S)			Bias (B)		Uncertainty ±(B + t₉₅S)					
	Percent of Reading	Unit of Measurement	Degree of Freedom	Percent of Reading	Unit of Measurement	Percent of Reading	Unit of Measure				
Test Section Total, TT1--TT2, °F	----	±0.27°F	100	----	±1.8°F	----	±2.3°F	0 to 60°F	Copper-Constantan Temperature Transducers	Sequential Sampling, Millivolt-to-Digital Converter, and Magnetic Tape Storage Data Acquisition System	Millivolt Substitution Based on the NBS Temperature versus Millivolt Tables
Plenum Temperature, TP1, °F	----	±0.27°F	100	----	+1.8°F	----	±2.3°F	-10 to 70°F			
Fuel Supply TF1--TF2, °F	----	± 0 27°F	100	----	±1.8°F	----	±2.3°F	60 to 80°F			
Fuel Injection TFI, °F	----	±0.27°F	100	----	±1.8°F	----	±2 3°F	20 to 80°F			
Holography Station Total, TH1--TH2, °F	----	±0.27°F	100	----	±2.2°F	----	±2.7°F	-5 to 60°F	Iron-Constantan Temperature Transducers		
Fuel Flow WFL1--WFL2, lb/min	± 0 11	----	20	±0.14	----	±0.37	----	12 to 15 lb/min	Turbine Volumetric Flow Transducers	Frequency-to-Voltage Converter onto Sequential Sampling, Millivolt-to-Digital Converter, and Magnetic Tape Storage Data Acquisition System	Frequency Substitution Based on the Standards Laboratory Determination of Transducer Water Volumetric Flow versus Frequency Output Relationship
Fuel Flow WFM1--WFM2, lb/min	+0.13	----	20	±0.21	----	±0.48	----	54 to 82 lb/min			
Fuel Flow WFH1--WFH2, lb/min	± 0 10	----	20	± 0 18	----	±0.39	----	250 to 295 lb/min			
Fuel Droplet Diameter, Microns	----	±4.25 Microns	31	----	+1.0 Microns	----	±9.5 Microns	10 to 100 Microns	Hologram	Hologram Reconstruction via Camera Vidicon onto CRT Monitor	In-Place Application of Physical Dimension to Determine Magnification Factor

*Ref. 4

AEDC-TR-74-117

Table 2. Summary of Test Conditions and Data

Date	Run	Data Point	Alt	VTS	WF	n_t	$\bar{d}$	$\bar{d}_m$	TF	PSA	PTA	TTA	VE	PSH	PTH	TTH	Configuration
			ft	knots	lb/min		micron	micron	°F	psia	psia	°F	knots	psia	psia	°F	
11/2/73	2	1	12000	198	0	*	*	*	68	9.32	9.97	26	205	9.20	9.69	26	0.652 ID Straight Fuel Nozzle
		2	11900	196	15.0	*	*	*	66	9.37	10.01	27	198	9.26	9.91	26	
		3	11900	193	14.5	*	*	*	68	9.36	9.99	26	197	9.25	9.89	25	
		4	11900	198	0	*	*	*	68	9.34	10.02	26	200	9.24	9.91	24	
		6	11900	197	74.0	60	19	26	68	9.37	10.02	27	199	9.25	9.91	26	
		6	11900	196	73.4	52	30	36	68	9.38	10.02	28	200	9.25	9.92	23	
		7	11900	196	145	*	*	*	88	9.37	10.02	28	199	9.25	9.91	24	
		8	11800	198	165	*	*	*	68	9.40	10.05	26	201	9.25	9.93	22	
11/5/73	3	1	11600	398	0	*	*	*	68	9.45	12.32	55	421	6.50	11.47	53	0.260 ID Straight Fuel Nozzle
		2	900	40	0	*	*	*	68	14.19	14.23	57	11	14.24	14.24	57	
		3	12000	364	14.3	*	*	*	66	9.32	11.93	54	420	6.40	11.33	52	
		4	12100	387	12.6	13	35	39	68	9.30	11.95	54	419	6.42	11.34	51	
		5	12100	313	13.5	15	27	30	66	9.31	11.99	43	314	8.96	10.61	42	
		8	12100	312	12.7	51	21	27	67	9.29	11.97	39	309	8.96	10.56	37	
		7	20000	405	12.6	27	22	24	67	6.75	9.04	26	444	5.86	6.40	24	
		6	18900	384	12.6	26	26	32	67	7.07	9.21	24	404	6.48	8.70	21	
		9	12000	213	12.6	37	29	33	67	9.34	10.11	25	184	9.43	10.01	24	
		10	11900	215	12.5	30	24	27	67	9.35	10.14	25	182	9.44	10.00	23	
		11	24900	389	12.9	26	27	30	87	5.47	7.22	11	405	5.06	6.66	8	
		12	24600	388	12.8	34	28	32	66	5.53	7.30	9	397	5.16	6.91	6	
11/8/73	4	1	11700	393	70.0	36	24	26	68	9.44	12.22	55	438	6.27	11.52	43	0.652 ID Straight Fuel Nozzle
		2	11700	398	70.0	*	*	*	67	9.42	12.25	57	440	6.26	11.36	51	
		3	11900	308	74.9	19	31	33	67	9.37	11.02	37	324	6.67	10.65	29	
		4	11900	302	72.2	*	*	*	67	9.36	10.96	34	317	8.92	10.63	28	
		6	19700	391	76.0	15	24	26	67	8.85	8.99	26	452	5.84	8.50	17	
		8	11800	197	73.1	*	*	*	67	9.39	10.04	27	198	8.25	9.90	23	
		7	11900	198	73.5	*	*	*	67	9.37	10.02	27	197	9.24	9.86	23	
11/14/73	5	1	11400	399	199	*	*	*	72	9.53	12.49	50	455	8.17	11.78	37	1.320 ID Straight Fuel Nozzle
		2	11400	407	283	36	21	22	73	9.54	12.61	53	466	7.96	11.71	39	
		3	11600	303	289	31	27	33	73	9.48	11.09	36	315	8.94	10.62	30	
		4	19300	389	289	41	33	35	73	6.95	9.09	26	449	5.63	8.44	16	
		5	23900	378	279	46	26	28	72	5.70	7.39	8	446	4.75	6.94	1	
		6	24100	388	286	41	30	35	72	5.65	7.45	7	467	4.54	6.90	0	
		7	19700	386	287	32	18	22	73	6.86	8.99	14	451	5.71	8.37	6	
		8	19900	390	61.9	76	34	37	72	6.79	8.91	23	441	5.80	8.29	15	
		9	19800	397	78.3	22	29	32	72	8.61	9.02	26	450	5.79	8.39	17	

*Hologram was not taken or was not usable

Table 2. Concluded

Date	Run	Data Point	Alt	VTS	WF	n_t	$\bar{d}$	$\bar{d}_m$	TF	PSA	PTA	TTA	VH	PSH	PTH	TTH	Configuration
			ft	knots	lb/min		micron	micron	°F	psia	psia	°F	knots	psia	psia	°F	
11/20/73	6	1	24700	395	54.8	31	23	27	75	5.50	7.36	5	470	4.49	6.87	-1	0.852 ID Straight Fuel Nozzle
		2	24300	382	68.9	51	19	22	75	5.80	7.35	5	449	4.70	6.91	-1	
		3	12000	203	66.1	21	33	38	75	9.33	10.03	22	207	9.17	9.89	19	
		4	11900	296	68.1	*	*	*	75	9.38	10.91	23	309	8.90	10.54	18	
		5	11600	406	67.6	*	*	*	75	9.40	12.48	42	484	7.72	11.73	34	
11/27/73	7	1	11900	201	69.3	23	29	33	76	9.37	10.06	19	208	9.17	9.89	16	0.852 ID Straight Fuel Nozzle and End Plates Installed
		2	11900	196	73.3	22	29	47	78	9.37	10.03	23	205	9.19	9.89	20	
		3	11800	292	72.2	46	26	30	78	9.36	10.90	23	314	8.90	10.62	19	
		4	11800	292	72.0	30	27	32	77	9.38	10.90	23	305	8.92	10.52	18	
		5	19900	391	73.8	23	21	22	77	6.79	8.93	23	473	5.57	8.44	14	
		6	20000	351	74.0	*	*	*	76	6.76	8.41	23	381	6.14	7.99	16	
		7	20000	345	74.0	11	21	24	76	6.76	8.35	23	377	6.15	7.95	18	
		8	11800	200	71.4	6	27	34	76	9.38	10.02	45	207	9.20	9.88	40	
		9	11800	372	71.0	*	*	*	78	9.39	11.83	54	406	8.43	11.17	45	
		10	11800	368	70.8	14	29	32	77	9.39	11.77	56	406	8.46	11.22	46	
12/6/73	8	1	23800	382	252	26	33	39	18	5.89	7.41	10	484	4.64	6.99	1	1.41 ID Canted Fuel Nozzle
		2	23900	379	285	34	24	31	19	5.70	7.44	7	459	4.88	7.01	-2	
		3	11400	203	291	*	*	*	22	9.54	10.24	28	210	9.33	10.08	22	
		4	19600	394	288	26	26	29	31	8.88	9.04	29	478	5.54	8.45	17	
		5	11700	301	293	*	*	*	39	9.42	10.99	39	323	10.63	8.86	30	
		6	11600	298	—	*	*	*	47	9.47	10.98	41	328	8.84	10.66	31	
12/12/73	9	2	23600	378	281	*	*	*	28	5.77	7.48	8	450	4.77	7.02	-2	1.320 ID Straight Fuel Nozzle
		3	23500	367	293	42	25	29	21	5.80	7.45	8	441	4.87	7.07	-3	
		4	11600	208	291	*	*	*	21	9.45	10.19	20	217	9.22	10.02	14	
		5	11600	209	291	*	*	*	34	9.46	10.21	22	218	9.22	10.03	16	
		6	11800	295	289	*	*	*	27	9.47	11.02	27	319	8.91	10.68	19	
		7	11700	300	289	13	36	40	33	9.42	11.00	33	319	8.86	10.61	23	
		8	11700	394	289	*	*	*	48	9.44	12.27	50	454	8.02	11.55	36	0.280 ID Straight Fuel Nozzle
		9	12000	202	13.0	31	29	38	32	9.33	10.02	25	202	9.18	9.86	24	
		10	12000	203	13.0	30	30	34	29	9.34	10.04	23	206	9.19	9.90	21	
		11	11900	294	13.1	18	27	31	29	9.38	10.86	33	309	8.93	10.55	30	
		12	12000	396	14.2	21	25	28	44	9.34	12.18	51	445	8.14	11.45	46	
		13	11900	399	13.0	22	27	29	48	9.35	12.21	54	448	6.12	11.43	49	

*Hologram was not taken or was not usable

39

AEDC-TR-74-117

Table 3. Summary of Hologram Data Taken at Planned Test Conditions

VTS, knots	Altitude, 1000 ft	WF=13 lbm/min		WF=70 lbm/min		WF=290 lbm/min		Totals	
		Number Made	Number Useful	Number Made	Number Useful	Number Made	Number Useful	Number Made	Number Useful
200	12	4	4	8	6	2	0	14	10
300	12	3	3	5	3	3	2	11	8
400	12	4	3	2	1	2	1	8	5
400	20	2	2	3	3	3	3	8	8
400	25	2	2	2	2	1	1	5	5
								—	—
							Totals	46	36

NOMENCLATURE

d	Fuel droplet diameter, microns
$\bar{d}$	Arithmetic average droplet diameter, microns
$\bar{d}_m$	Mass-weighted average droplet diameter, microns
d_o	Area-volume average droplet diameter, microns
n	Number of fuel droplets
n_t	Total number of droplets
PSA	Average static airflow pressure at fuel injection station, psia
PSH	Average static airflow pressure at holography station, psia
PTA	Average total airflow pressure at fuel injection station, psia
PTH	Average total airflow pressure at holography station, psia
Q_a/Q_ℓ	Volumetric flow rate ratio (air to liquid)
TF	Average fuel temperature, °F
TTA	Average total airflow temperature at fuel injection station, °F
TTH	Average total airflow temperature at holography station, °F
VH	Average airflow velocity at holography station, knots
VTS	Average airflow velocity at fuel injection station, knots
WF	Average fuel mass flow rate, lbm/min
μ	Viscosity of liquid
ρ	Density of liquid
σ	Surface tension of liquid
Ψ	Relative frequency of occurrence of droplet size